BARENTS PROJECT 2013

Geological and geophysical studies in the Nunasvaara, Saarijärvi and Tjårrojåkka areas, northern Norrbotten

Edward P. Lynch, Johan Jönberger, Stefan Luth,
Susanne Grigull & Olof Martinsson

February 2014

SGU-rapport 2014:04

SGU
Sveriges geologiska undersökning
Geological Survey of Sweden

Cover: Aerial view of the boreal landscape at Saarijärvi, Norrbotten. View looking east with lake Kaalasjärvi on the right. Foto: Edward Lynch.

Sveriges geologiska undersökning
Box 670, 751 28 Uppsala
tel: 018-17 90 00
fax: 018-17 92 10
e-post: sgu@sgu.se
www.sgu.se

CONTENTS

SAMMANFATTNING

Den här rapporten är en sammanställning av de berggrundsgeologiska och geofysiska fältaktiviteter som har bedrivits under 2013 inom nyckelområdena Nunasvaara, Saarijärvi och Tjårrojåkka. Nyckelområdena ligger nära Kiruna och området är en av Europas viktigaste provinser för metallförekomster av järn, guld och koppar. Rapporten innehåller en redogörelse för de geologiska och geofysiska observationer, mätningar och provtagningar som har gjorts i de här områdena vars geografiska utbredning finns i figur 1. Fältobservationer och provtagningar spelar en avgörande roll för geologisk kartläggning och utgör grundläggande information för framtida undersökningar. Fältarbetet i de här områdena genomfördes under 32 dagar under perioden juni–augusti 2013.

INTRODUCTION

This report provides a summary of SGU's field activities conducted during the summer of 2013 in Norrbotten county, Sweden. The work forms part of SGU's ongoing Barents Project (2012–2015) which is focused on targeted geologic investigations within 14 key areas in northern Norrbotten. The broad aim of the project is to further our understanding of unresolved stratigraphic, structural and metallogenic processes in the region through the integration of new geological, geophysical and geochemical data. An overview of work conducted in the Nunasvaara, Saarijärvi and Tjårrojåkka key areas located close to Kiruna is presented (Fig. 1). The Kiruna district, and northern Norrbotten as a whole, is recognised as one of Europe's important mining and exploration regions (e.g. Bilström et al. 2010, Martinsson & Wanhainen 2013).

The report is divided into three sections corresponding to the different study areas, and each section begins with a brief summary of the area's geological setting. Following this, an overview of new bedrock observations and measurements (structural, geophysical) is presented. Outcrop-scale lithological features and their associated geophysical characteristics are emphasised. Bedrock sampling in the study areas was also performed and provides a basis for ongoing laboratory

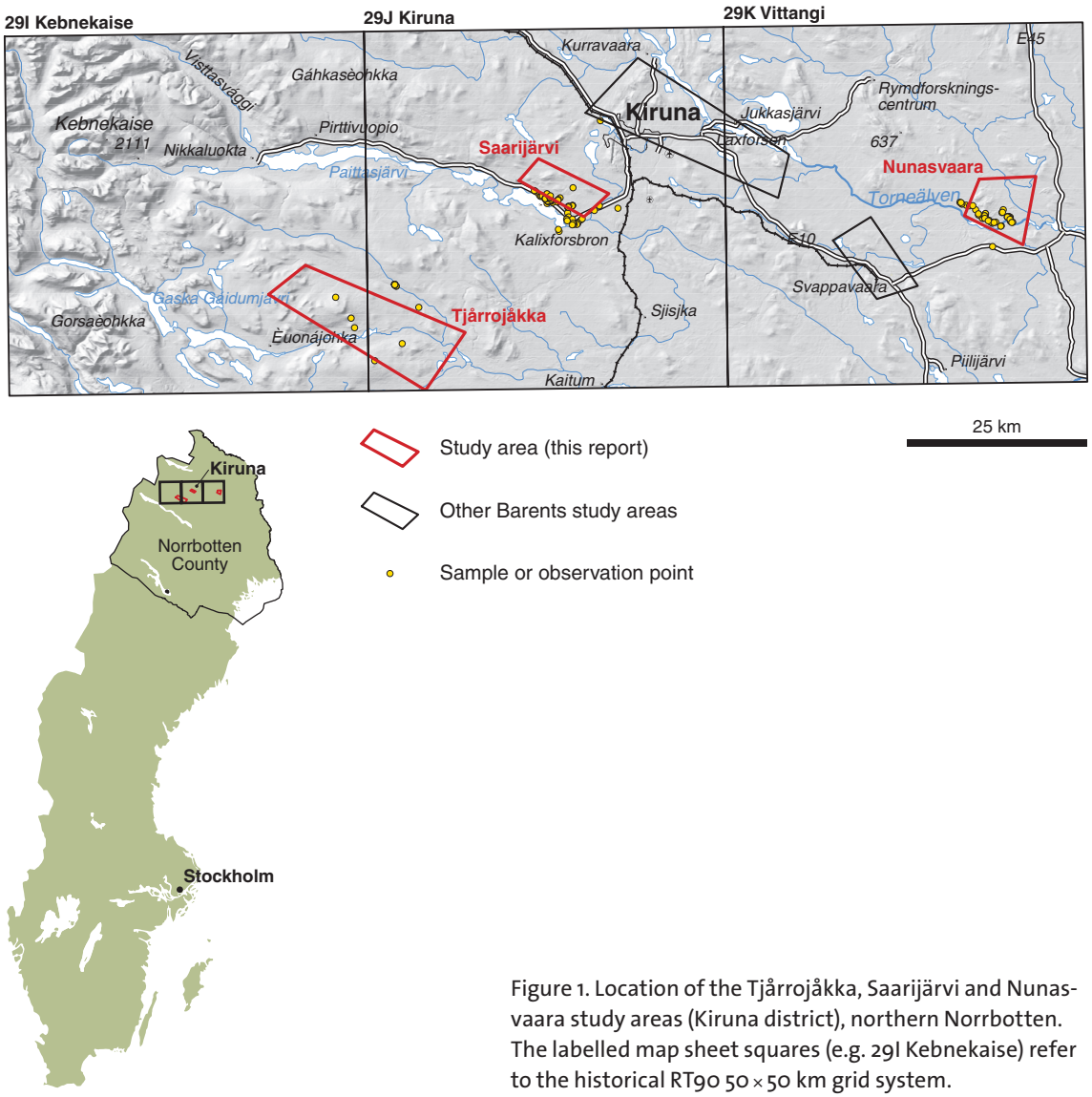

Figure 1. Location of the Tjårrojåkka, Saarijärvi and Nunasvaara study areas (Kiruna district), northern Norrbotten. The labelled map sheet squares (e.g. 29I Kebnekaise) refer to the historical RT90 50 × 50 km grid system.

based investigations (e.g. mineralogy, lithogeochemistry, geochronology). Field work was undertaken over 32 days spread across the summer months from June to August.

The three investigated areas are all underlain by Precambrian bedrock that forms part of the larger Norrbotten lithotectonic domain of northern Sweden (Fig. 2). This geologic region incorporates both Archean and Paleoproterozoic crust that acquired a shared tectonothermal history between approximately 2.0 and 1.7 Ga during the Svecokarelian orogeny (Stephens & Weihed 2013). The majority of the described rocks have been metamorphosed to upper greenschist facies conditions (e.g. Bergman et al. 2001). In this report, the prefix meta- has been omitted from outcrop and lithological descriptions for brevity (i.e. basalt instead of metabasalt). Coordinates quoted in the main text and shown on maps and in figure captions correspond to the Sweref99 coordinate system (northing and easting values, respectively).

FIELD ACTIVITIES AT NUNASVAARA

The Nunasvaara key area (NKA) is located about 10 km west of Vittangi (Figs. 1 and 3). The geology of the Nunasvaara key area has been described in earlier SGU reports by Geijer (1918), Ödman (1957), Eriksson & Hallgren (1975) and Gustafsson (1993), while bedrock mapping is covered by SGU's 1:50 000-scale Af series (Af 13–16 Vittangi, Eriksson & Hallgren 1975). The area is best known for its schist-hosted graphite deposits (e.g. Shaikh 1972, Gerdin et al. 1990) and skarn-type iron mineralisation (e.g. Frietsch 1997). A compilation of existing bedrock mapping, geochronology, geochemistry and geophysical data for the area is presented in Lynch & Jönberger (2013a).

The Nunasvaara key area contains a greenstone sequence consisting of basalts, tuffs, intercalated metasedimentary rocks (quartzite, schist, marble, graphitic schist) and doleritic sills (Figs. 3 and 4). These greenstones form part of the Vittangi greenstone group which covers the broader Svappavaara, Vittangi and Soppero areas. The greenstones are considered to be an eastern extension of part of the greenstone stratigraphy established in the Kiruna area (e.g. Martinsson 1997), and have been correlated to a lower to middle stratigraphic position within the Kiruna greenstone group (e.g. Martinsson 1993, 1995). Important lithological differences and facies variations exist between these areas which has probably influenced mineralisation at Nunasvaara (e.g. Martinsson 1993). Intrusive rocks in the area include: (1) Haparanda-type gabbroids, diorites and granitoids (c. 1.90–1.86 Ga), (2) broadly contemporaneous Perthite-monzonite-type gabbroids and granitoids (c. 1.88–1.86 Ga) and (3) younger Granite-pegmatite suite granites (or "Lina-type", c. 1.81–1.74 Ga).

Bedrock observations, structural measurements, bedrock sampling and ground geophysical measurements (magnetometry, VLF electromagnetometry) were made along a west-north-west orientated profile that transects the greenstone stratigraphy (point symbols in Fig. 3). The profile runs approximately orthogonal to deformed bedding within a north-north-east orientated antiform–synform structure (Fig. 4). The eastern end of the sampling profile is located in lowermost greenstone basalts (7524221/773437), while the western end is located in uppermost altered and crystalline tuff (7526220/766614). Thus, the profile provided an opportunity to sample a relatively conformable sequence of greenstone-related rock types.

The aim of the field work was to further characterise the various greenstone units and better constrain local and regional stratigraphic relationships. Ongoing petrographic, lithogeochemical and geochronological analyses will provide additional insight into greenstone petrogenesis and facilitate regional correlations with other greenstone sequences in Norrbotten. Observations and sampling focusing on hydrothermal alteration and mineralisation processes were also done.

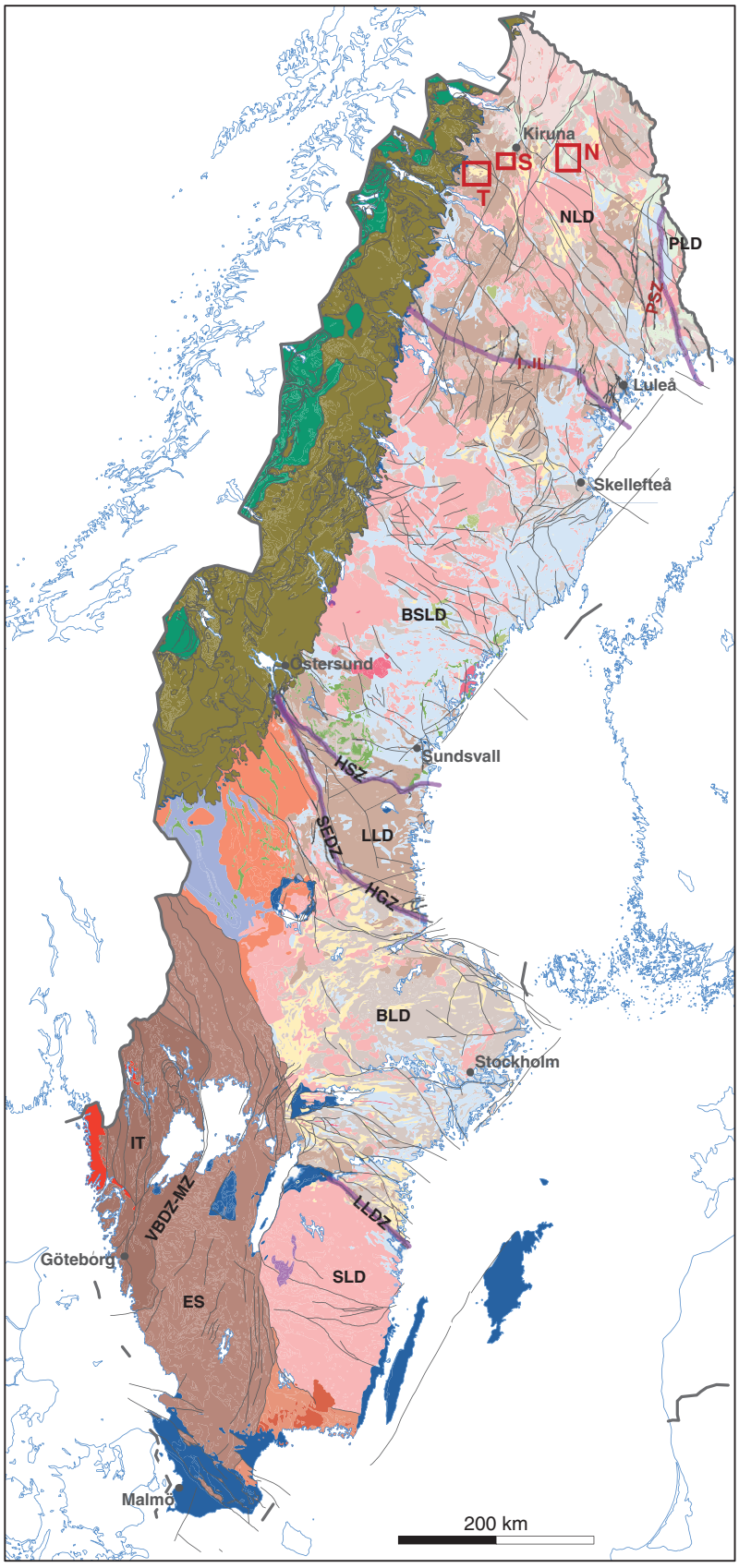

BLD	Bergslagen lithotectonic domain
BSLD	Bothnia-Skellefteå litho-tectonic domain
ES	Eastern Segment
HGZ	Hagsjö Gneiss Zone
HSZ	Hasselö Shear Zone
IT	Idefjorden terrane
LJL	Luleå–Jokkmokk line
LLD	Ljusdal lithotectonic domain
LLDZ	Loftahammer-Linköping deformation zone
NLD	Norrbotten lithotectonic domain
PLD	Peräpohja lithotectonic domain
PSZ	Pajala shear zone
SEDZ	Storsjön–Edsbyn Deformation Zone
SLD	Småland lithotectonic domain
VBDZ-MZ	Värmlandsnäs-Bua deformation belt including the Mylonite Zone
	Boundary between lithotectonic domains inside the Sveco-karelian orogen

Figure 2. Lithotectonic map of Sweden showing the position of the Tjårrojåkka (T), Saarijärvi (S) and Nunasvaara (N) key areas within the Norrbotten lithotectonic domain (modified after Stephens & Weihed 2013).

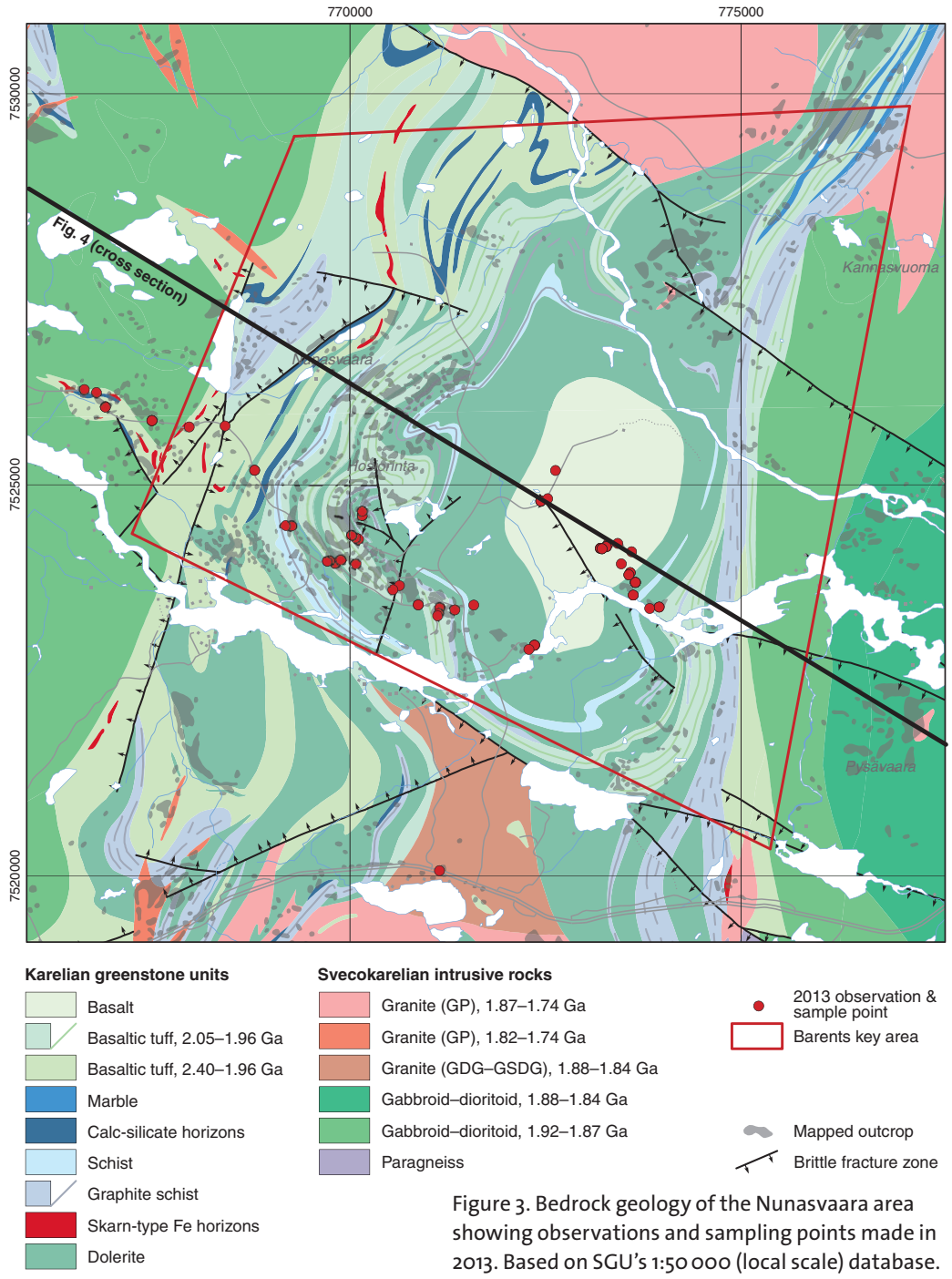

Figure 3. Bedrock geology of the Nunasvaara area showing observations and sampling points made in 2013. Based on SGU's 1:50 000 (local scale) database.

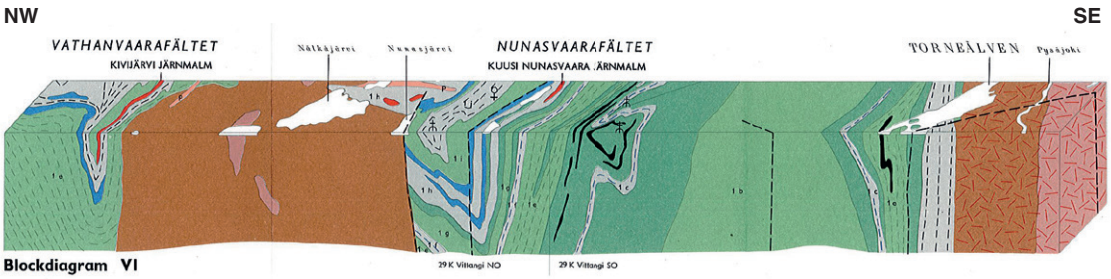

Figure 4. Cross-section through greenstone and intrusive rocks at Nunasvaara, as presented by Eriksson & Hallgren (1975). The profile corresponds to the diagonal line drawn in Fig. 3. Note that the colour scheme of the cross-section does not exactly correspond to the bedrock map colours shown in Figure 3.

Outcrop and petrographic features of greenstone-related units

The lowermost unit in the greenstone sequence (Lower greenstone formation, Eriksson & Hallgren 1975) is a dark grey to greenish grey, aphanitic, amygdaloidal basalt that crops out across several scattered, flat-lying exposures in the centre of the study area (Fig. 3). In general, it has a massive, non-foliated appearance without conspicuous banding or layering (Fig. 5a–b). Although bedding contacts are not well exposed, some outcrops display somewhat bulbous, polygonal forms, suggesting flow bedding thicknesses of c. 0.7–2 m. Gustafsson (1993) reports a total thickness of c. 1.2 km for this basalt unit, although the contact with the underlying unit (Tjärro quartzite formation) does not occur in the area. Likewise, true thicknesses of the various greenstone volcanosedimentary units as a whole are difficult to establish due to the intrusion of mafic sills in the sequence.

A conspicuous feature of the basalt is the presence of amygdules, which impart a spotted appearance to the rock (Fig. 5b–d). The amygdules are generally oblate to locally elongate or irregular (pipe-like), and typically range from 0.3 cm to 1.5 cm in size. Amygdules predominantly consist of dark greenish grey, amphibole-rich cores (actinolite, hornblende?) with pale, creamy white albite±scapolite rims (Fig. 5b–c). Locally, the cores have a paler green appearance, suggesting the presence of epidote±chlorite. In som places the amygdules consist of creamy white albite±scapolite spots without dark coloured, amphibole-rich cores (Fig. 5d). Biotite, pyrite and hematite amygdules have previously been reported from basalts in the Nunasvaara area (Eriks-

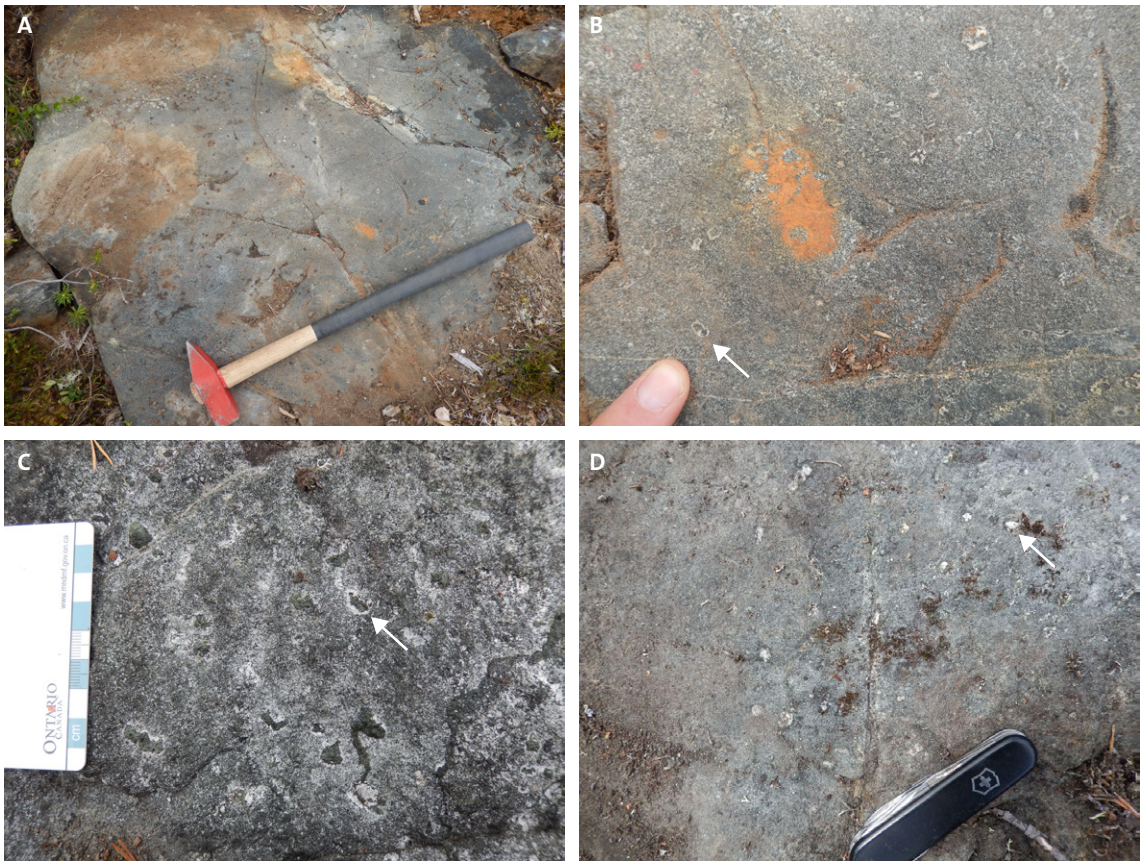

Figure 5. Massive, thickly-bedded basalt at Nunasvaara, c. 600 m north of Torneälven (7524214/773323). **A.** Typical outcrop with a flattened, bulbous, polygonal morphology (7524146/773598). **B–C.** Centimetre-scale amygdules (arrows) consisting of an amphibole-rich core and albite±scapolite rims (7524146/773598, 7524254/773422). **D.** Examples of albite-carbonate(?)-epidote-rich amygdules (arrow), locally with darker (amphibole?), diffuse rims (7524146/773598).

son & Hallgren 1975). Measured magnetic susceptibility values of basalt outcrops ranged from 101 to 17 500 × 10^{-5} SI, with an average value of 5 072 × 10^{-5} SI (n=40). The broad range in the susceptibility values is probably a consequence of variable magnetite-bearing alteration and veining that locally affects the basalt (see below).

Based on a limited number of lithogeochemical analyses (n=12, combined ICP-AES and ICP-MS analyses), the amygdaloidal basalt at Nunasvaara has a subalkaline, high-Fe tholeiite composition and is relatively low in K_2O, with values ranging between 0.54 and 1.56 wt.% (Fig. 6). These preliminary data, combined with the general petrographic character of the basalts, indicate that the basalts in Nunasvaara are similar to basalt flows in the Kiruna area that occupy a lower to middle stratigraphic position within the Kiruna greenstone group (e.g. Pikse formation, cf. Martinsson 1993, 1997). The new lithogeochemical data are also broadly similar to preliminary results presented by Lager & Loberg (1990) on Nunasvaara greenstone rocks.

A relatively thick sequence (c. 2 km) of laminated tuffs lie stratigraphically above the amygdaloidal basalt (Figs. 7–8). Using the local stratigraphic nomenclature (Eriksson & Hallgren 1975), this unit forms part of the Upper greenstone formation. In general, the tuffs have a banded, alternating dark grey to pale grey appearance, are fine- to medium-grained (0.1–2 mm) and occur as parallel, laterally continuous, planar to wavy, thin to medium beds ranging between c. 3 cm and 50 cm in thickness (Fig. 7a–b). Along the mapped profile (Fig. 3), the tuffs dip steeply (c. 80–90°) towards west-south-west, which coincides with the interpreted younging direction of the sequence (cf. Eriksson & Hallberg 1975). Within individual beds, the tuff has a stratified appearance and contains planar to wavy, parallel to sub-parallel, laterally continuous laminae that are 0.1–1 cm thick (Figs. 7c and 8). In some outcrops, the rock is entirely composed of thin (<1 cm) planar to wavy laminae (Fig. 7c). Higher in the sequence, the tuffs have a more crystalline, non-laminated appearance (Fig. 7d). This more crystalline variety occurs adjacent to a large quartz monzodiorite intrusion (discussed below), along with zones of intense amphibole-sulphide alteration and skarnification. Thus, Svecokarelian-cycle magmatism may have provided a mechanism for localised recrystallisation and hornfels alteration of the volcanic rocks.

Other features of the basaltic tuff include the presence of chert-like nodules and bands, granular (coarser) horizons with possible lapilli-type features, and linear zones of paler volcanic material suggesting a more intermediate composition. At one location (7524051/ 769888), dis-

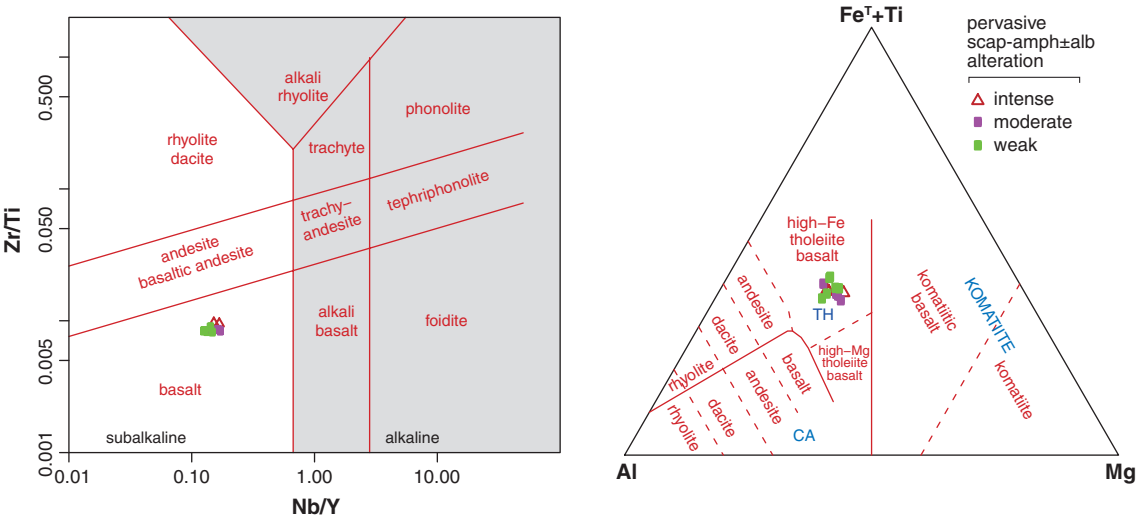

Figure 6. Lithogeochemical classification plots for volcanic rocks (Pearce 1996, Jensen 1976) showing the position of variably scapolite-altered amygdaloidal basalts from Nunasvaara.

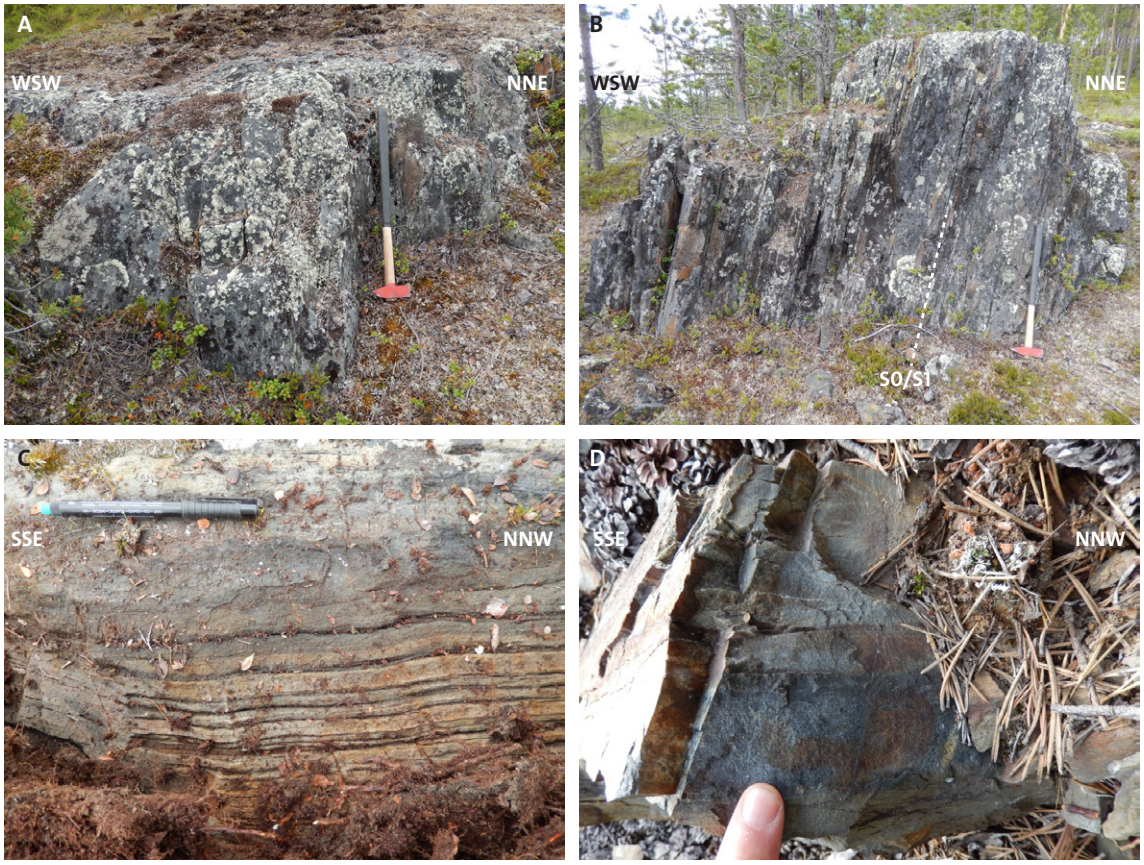

Figure 7. Basaltic tuffs at Nunasvaara. **A.** Typical outcrop of steeply dipping laminated tuff (7524028/769710). **B.** Laminated tuff representing hanging-wall rocks of the Nunasvaara graphite deposit. A penetrative foliation (S1) is present and is generally sub-parallel to primary laminae or bedding (S0, 7523996/770076). **C.** Example of a laminated tuff displaying alternating (rhythmic) banding and compositional (mafic–intermediate) variation (7524051/769888). **D.** Crystalline tuff adjacent to skarn-type iron mineralisation (7525754/768403).

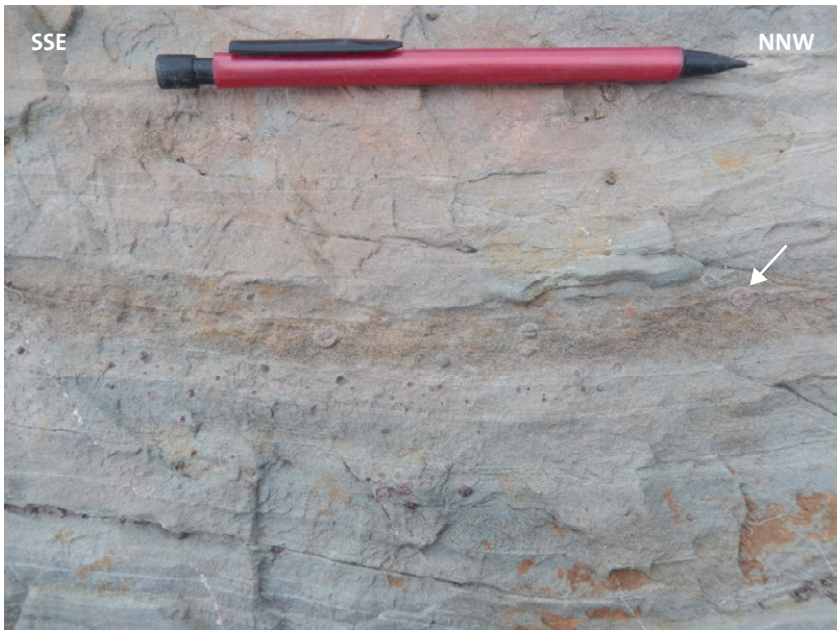

Figure 8. Laminated basaltic tuff containing subhedral to euhedral, fine- to medium-grained (<3 mm), almandine garnet (arrow, 7524051/769888).

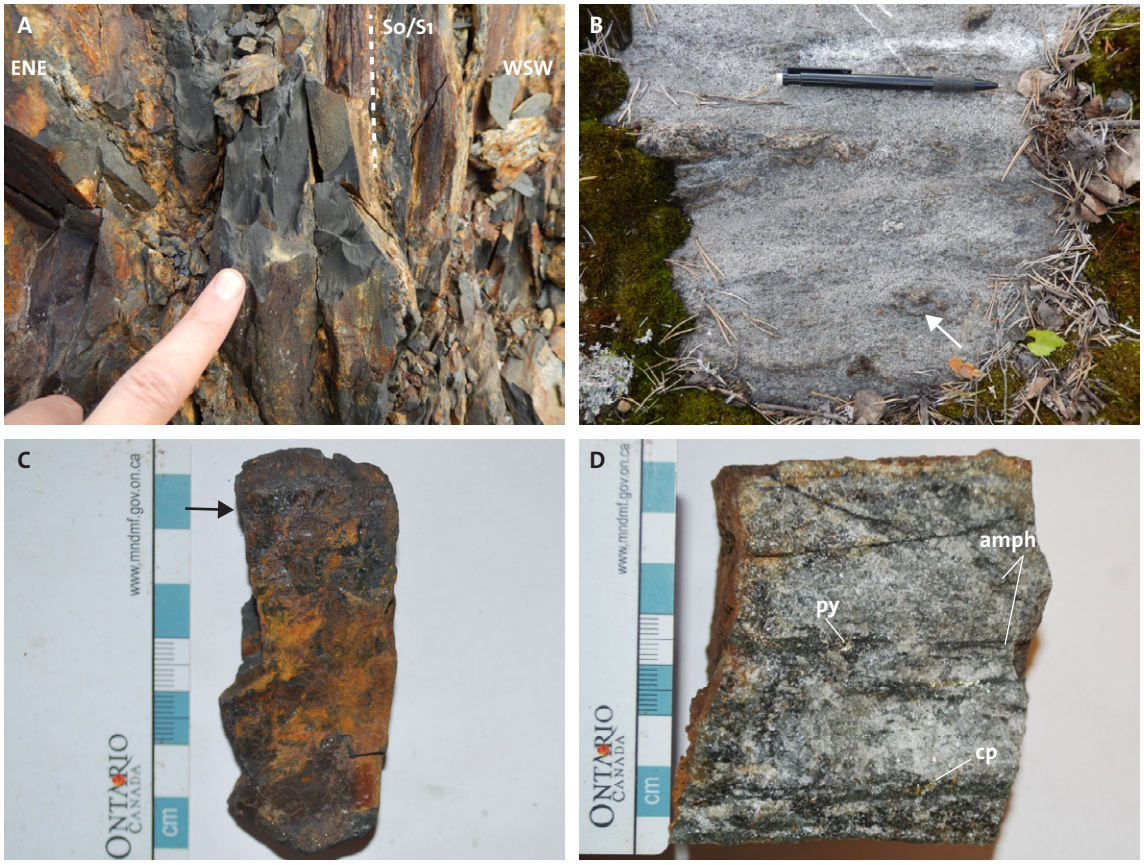

Figure 9. Metasedimentary horizons at Nunasvaara. **A.** Graphite schist at the Nunasvaara deposit. The penetrative schisosity (S1) is sub-parallel to bedding (S0, 7524309/770109). **B.** A siliceous limestone (marble) unit with fragments and clots of possibly volcanic material (arrow) forming discontinuous bands (7524615/769180). **C.** Hand sample of banded ironstone from the Nunasvaara area (7524620/769174). Thin laminae indicated by arrow. **D.** Hand sample of a sulphide-bearing chert horizon (7526180/766759).

seminated almandines occur within several distinct bands that are up to several centimetres thick (Fig. 8). The garnets are generally subhedral to euhedral, dark red to greyish red, fine- to medium-grained (c. 0.2–0.8 cm) and appear to preferentially occur within darker brown to rusty brown horizons with a more clay-like appearance (Fig. 8).

Measured magnetic susceptibility values from tuff outcrops ranged from 33 to $22\,500 \times 10^{-5}$ SI, with an average value of $3\,671 \times 10^{-5}$ SI (n=48). The broad range in the susceptibility values may be a consequence of variable magnetite-bearing alteration, veining and brecciation that locally affects the tuffs (see below).

The greenstone sequence at Nunasvaara contains several intercalated metasedimentary units and horizons. A transitional sequence termed the Lower sedimentary formation (local nomenclature) is located stratigraphically between the previously described basalt and tuff units. It consists of a relatively thin zone (c. 300–400 m) of gneissose schist and graphite schist. This formation hosts the Nunasvaara graphite deposit (7524309/770109). At this deposit, the host rock is a dark grey to black, fine-grained (<0.5 mm), crenulated, graphite-rich schist (Fig. 9a). In outcrop, it displays a strongly developed, sub-vertical spaced cleavage and planar schistose fabric (S1) that is orientated sub-parallel to bedding contacts with both hanging wall (tuff) and footwall (dolerite) rocks (e.g. Fig. 10c). Late-stage, epigenetic quartz-carbonate veinlets containing pyrite and galena also occur in the area.

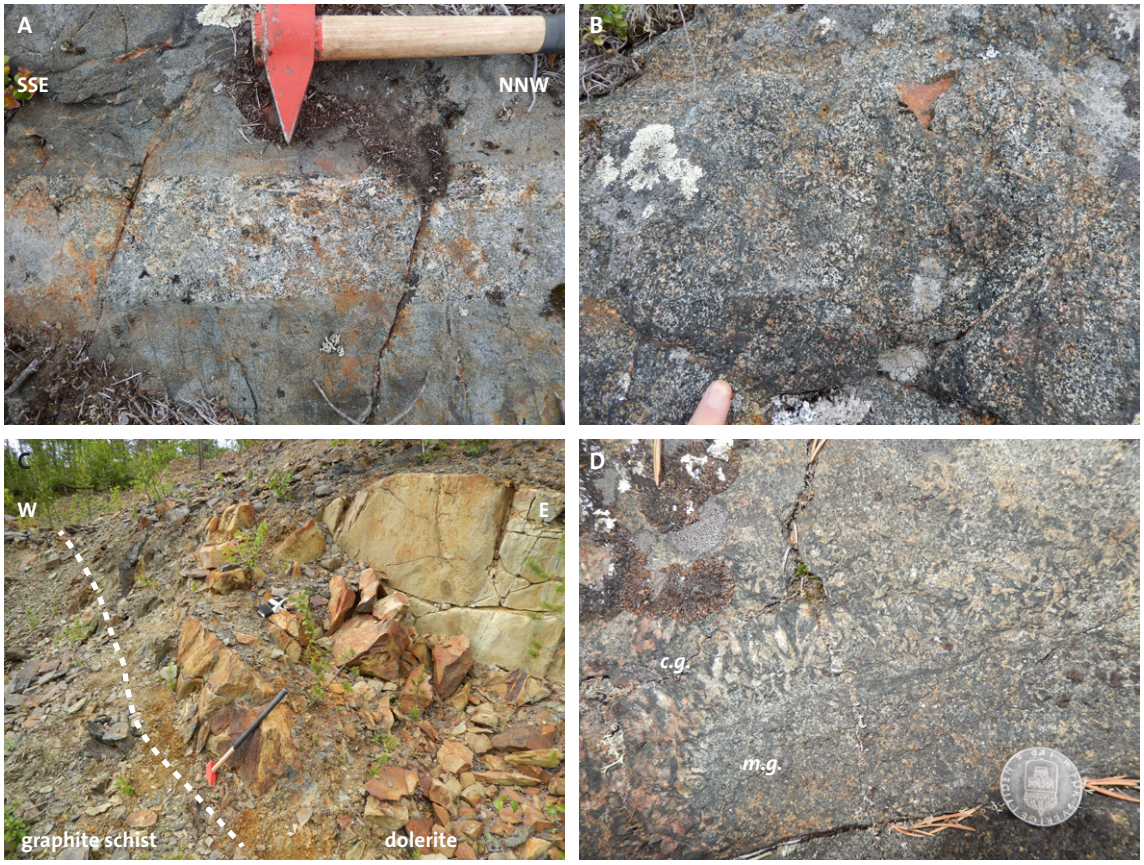

Figure 10. Doleritic intrusive rocks in the Nunasvaara area. **A.** Example of a relatively narrow (c. 25 cm) dolerite sill cross-cutting hornfelsed tuff (7524010/769811). **B.** Typical scapolite-amphibole-altered appearance of a dolerite sill (7523715/770631). **C.** Contact between dolerite and schist in the footwall of the Nunasvaara graphite deposit (7524309/770109). **D.** Example of grain size variation (medium- to coarse-grained) in a dolerite sill (7523469/770870).

Additional sedimentary units are found as intercalations within the Upper greenstone formation (i.e. basaltic tuffs previously described) and within an overlying metasedimentary package termed the Upper sedimentary formation (Eriksson & Hallgren 1975). This latter unit consists of crystalline tuffaceous rocks (e.g. Fig. 7d) that contain horizons of siliceous limestone (Fig. 9b), quartz-rich units (chert or metaarenite?), banded ironstone (Fig. 9c) and stratiform zones of intense alteration, skarn-type iron (e.g. Kuusinunasvaara deposit north-west of the key area) and skarn-related sulphide mineralisation. In the skarn-sulphide areas, the bedrock typically has an intensely rusted appearance displaying pervasive and vein-related amphibole and silica alteration with associated pyrite, chalcopyrite and magnetite (Fig. 9d).

Doleritic intrusions are conspicuous features of the greenstone sequence at Nunasvaara (Fig. 10). They occur as sub-volcanic, sill like bodies that intrude formational contacts and zones of lithological contrast (cf. Fig. 3). They typically range in thickness from c. 0.3 m to 100 m, although a relatively thick doleritic body (c. 300–400 m) is encountered at the centre of the study area (Figs. 3 and 4). Contacts (where visible) are sharp, planar and parallel (Fig. 10a). The majority of sills are deformed and folded in a ductile manner, mimicking the parasitic open fold deformation seen in the tuffs and metasedimentary rocks along the limbs of the north-north-east orientated antiform–synform train (Fig. 3). Axial planes are sub-vertical, generally orientated west-north-west to north-west and plunge steeply to the west-north-west. A U-Pb age determi-

nation on titanite from an altered dolerite sample from the eastern limb of the Nunasvaara antiform gave an age of 1903±8 Ma (Smith et al. 2009). This age provides a minimum age constraint for hydrothermal alteration in the area.

The dolerite is typically dark grey to dark greenish grey, fine- to medium-grained (c. 0.5–5 mm), intercrystalline and massive. Locally, it grades into coarser crystalline zones (c. 10 mm) that have a gabbroic appearance (Fig. 10d). The primary mineralogy is pyroxene, plagioclase feldspar, possibly some olivine, and magnetite. The majority of outcrops display a moderate to intense, pervasive, actinolite-scapolite-albite-magnetite±titanite alteration (Fig. 10b, see below). Minor quartz veinlets and patches also occur. Dolerite outcrops are generally magnetic reflecting the presence of disseminated, tabular patches and grains of magnetite (c. 0.3–5 mm in size) intergrown within the mafic matrix. Magnetite also occurs as inclusions within pyrite (intergrowths). On weathered surfaces magnetite displays light grey rims and microgranular staining that may reflect rutile- or brookite-type replacement of ilmenite inclusions. Rare disseminated pyrite overprints pyroxene and actinolite. Secondary hematite-goethite replaces magnetite and pyrite.

The measured magnetic susceptibility values of dolerite outcrops ranged from 39×10^{-5} to $35\,200 \times 10^{-5}$ SI, with an average value of $6\,068 \times 10^{-5}$ SI (n=104). The broad range in susceptibility values is a likely consequence of the relatively high magnetite content of the rock, along with variable magnetite-bearing alteration and veining that locally affects it (see below).

Hydrothermal alteration and mineralisation processes in the greenstones

The greenstone sequence at Nunasvaara has been affected by hydrothermal alteration and veining which overprints the primary mineralogy and textures. Many outcrops contain planar, sheeted to stockwork-type actinolite-magnetite±albite±scapolite veins. Hydrothermal breccias also occur at several locations. This section describes some of the observed features and characteristics of the alteration and veining that affect the greenstones previously described (i.e. basalt, tuff, dolerite). An example of an amphibole-rich hydrothermal breccia is also discussed.

Outcrops of tholeiitic basalt (Lower greenstone formation) in the centre of the study area display moderate to intense alteration (Fig. 11). Examples of "least altered" basalt are rare (e.g. Fig. 11a). The majority of outcrops are affected by an early, pervasive, scapolite-amphibole±albite±magnetite±pyrite assemblage that has a persistent, pale grey, fine-grained, speckled appearance on exposed surfaces (Figs. 5b, 12a–b). The intensity of alteration varies from weak (patchy) to moderate and intensely pervasive (Fig. 11). Weakly to moderately altered basalt contains fine-grained scapolite±albite (replacing plagioclase) along with fine-grained actinolite patches and halos (replacing pyroxene?), sometimes associated with disseminated pyrite (Fig. 11b–c). Where alteration is intense, scapolite porphyroblasts up to 0.5 cm in size occur within an amphibole-rich matrix (Fig. 11f).

Hydrothermal veining and vein-related (selective) alteration also occurs in the basalt and cross-cuts the earlier pervasive scapolite alteration. Two main vein types are recognised: albite±scapolite veins (Fig. 12a–b), generally without alteration halos, and actinolite±magnetite veins with variably developed albite alteration halos (Figs. 12c–b). The latter vein type is the most common. The albite veinlets are typically thin (<1 cm), planar to wavy or irregular. While generally associated with actinolite-magnetite veins, they commonly occur within earlier fractures and are cross-cut by the actinolite-magnetite veins. This suggests the albite-scapolite veins may represent an early stage of brittle fracturing and fluid flow associated with the pervasive scapolite-amphibole±albite alteration.

Actinolite±magnetite veins with variably developed albite alteration halos typically range from 0.3 cm to 2 cm in thickness. They are planar to locally wavy or irregular and do not dis-

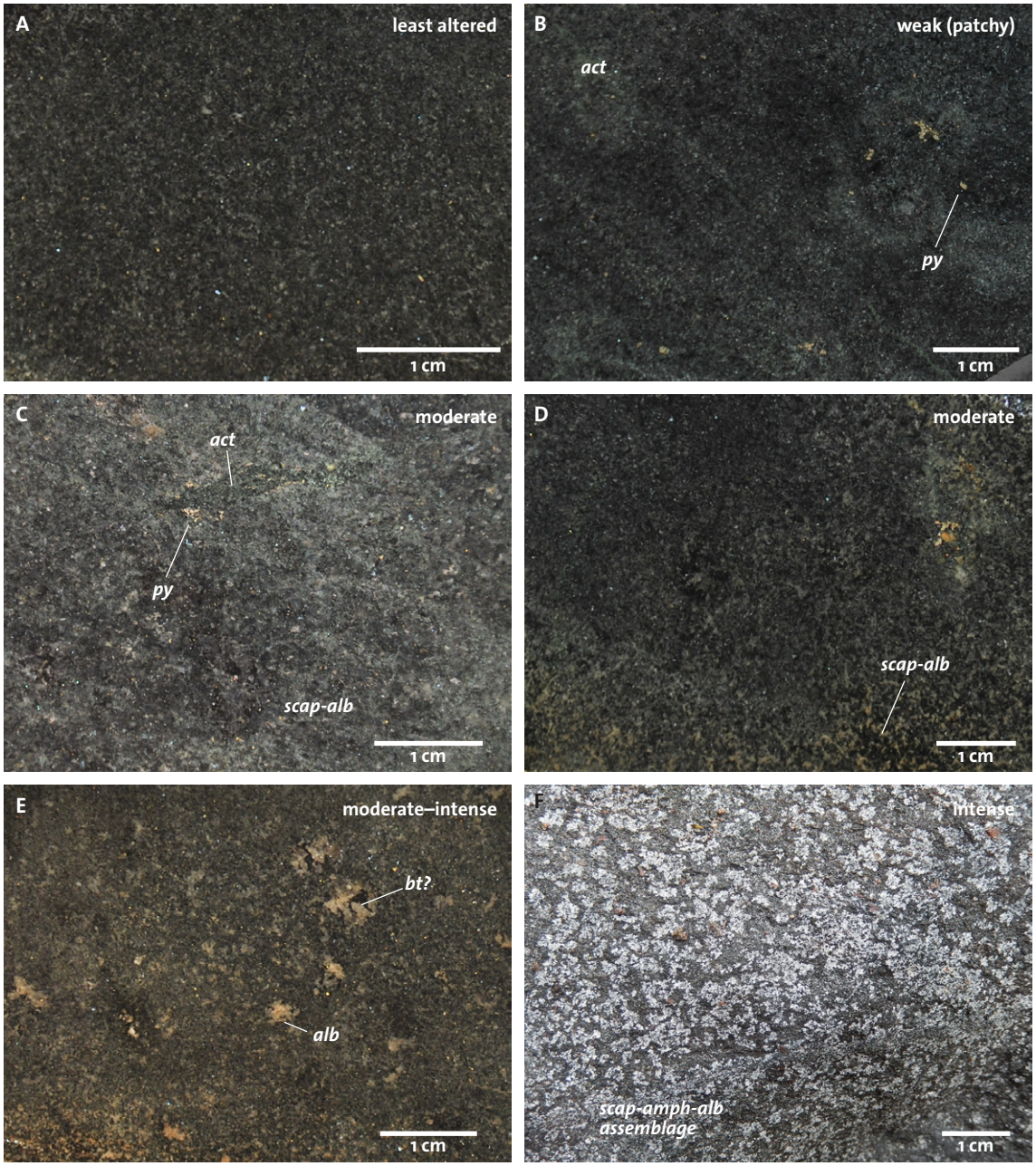

Figure 11. Relative alteration grades of metabasalt as seen on wet, cut slabs (except F). All scale bars are 1 cm. **A.** Least altered, aphanitic basalt. Magnetite-bearing. **B.** Patchy actinolite-albite alteration. Notice actinolite halo surrounding sulphides. **C–D.** Moderate amphibole-scapolite-albite alteration. **E.** Moderate to intense, pervasive scapolite-amphibole-albite alteration. Albite occurs as small clots and fills amygdules. **F.** Intense, pervasive scapolite porphyroblasts on a dry, outcrop surface (7524240/773291).

play a preferred orientation (Fig. 12c). Vein-hosted actinolite is generally fine-grained, granular and massive. Locally, actinolite veins have a strong magnetism, indicating the presence of fine-grained magnetite. Some veins, however, are non-magnetic while the adjacent wall-rock is often anomalously magnetic regardless of the presence of an albite halo. This suggests that magnetite mineralisation is either variably developed within actinolite veins, or that the remobilisation and concentration of primary "wall rock" magnetite may have occurred during vein formation.

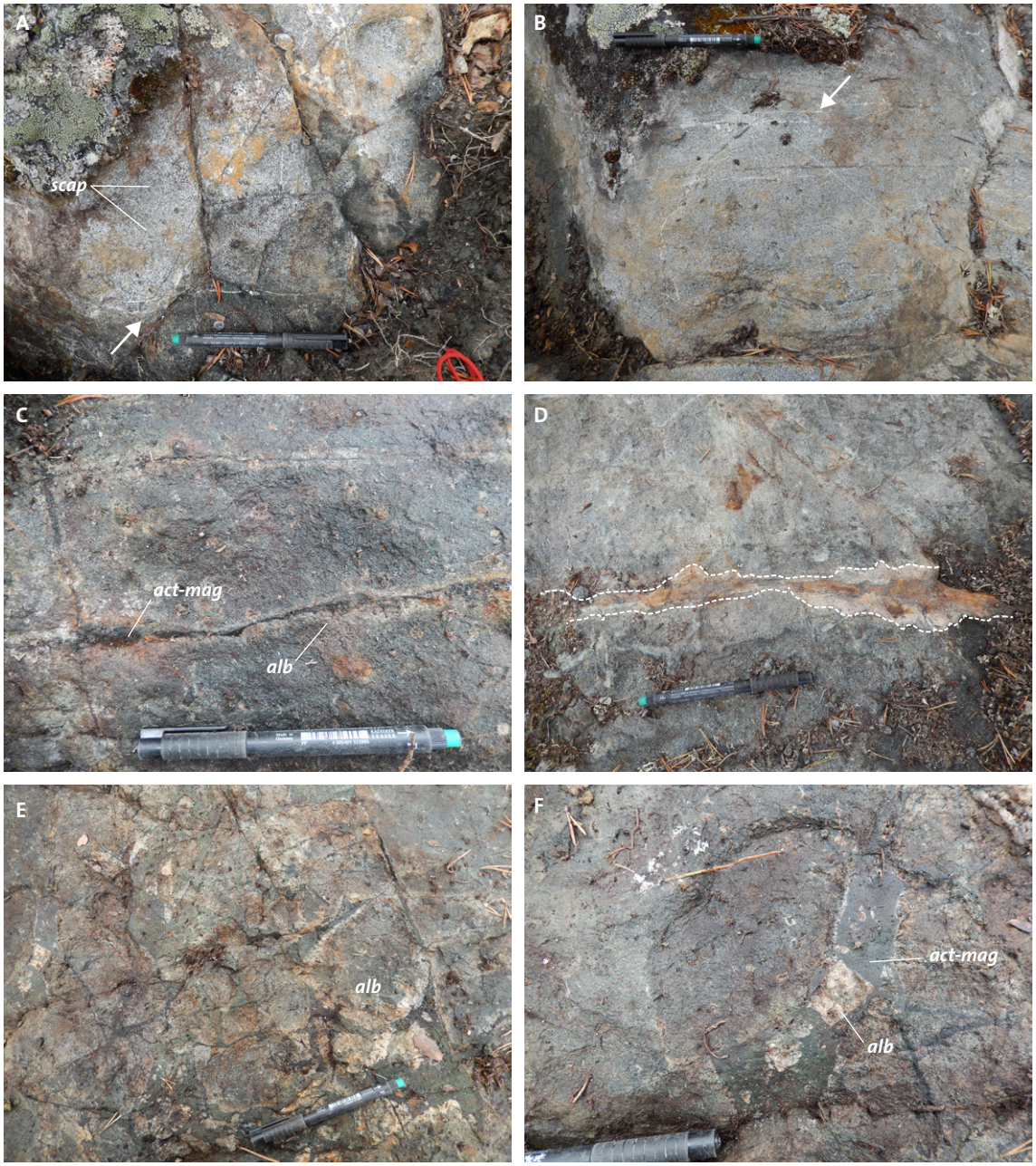

Figure 12. Outcrop-scale examples of basalt alteration and veining (ELH130060). **A–B.** Pervasive, moderate to intense scapolite-amphibole alteration. Albite±scapolite veinlets (arrows) also occur (7524190/773201). **C–D.** Actinolite-magnetite veinlets with albite alteration halos (dashed outline in D). Secondary, patchy hematite±goethite occurs after magnetite and pyrite (7524190/773201). **E–F.** Moderate to intense stockwork- and breccia-style actinolite-magnetite-albite veining (7524190/773201).

Vein-related albite alteration halos are continuous to locally patchy, or are sometimes absent (Fig. 12b). In some cases, the albite halo dominates the vein structure with a remnant, actinolite±magnetite veinlet forming a thin central channel (Fig. 12d). Secondary hematite±goethite commonly occurs within veins and alteration halos (after magnetite). Locally, actinolite-magnetite veining is intensely developed and imparts a breccia or stockwork appearance to the rock (Fig. 12e–f). Fragments of basalt material within these stockwork zones appear

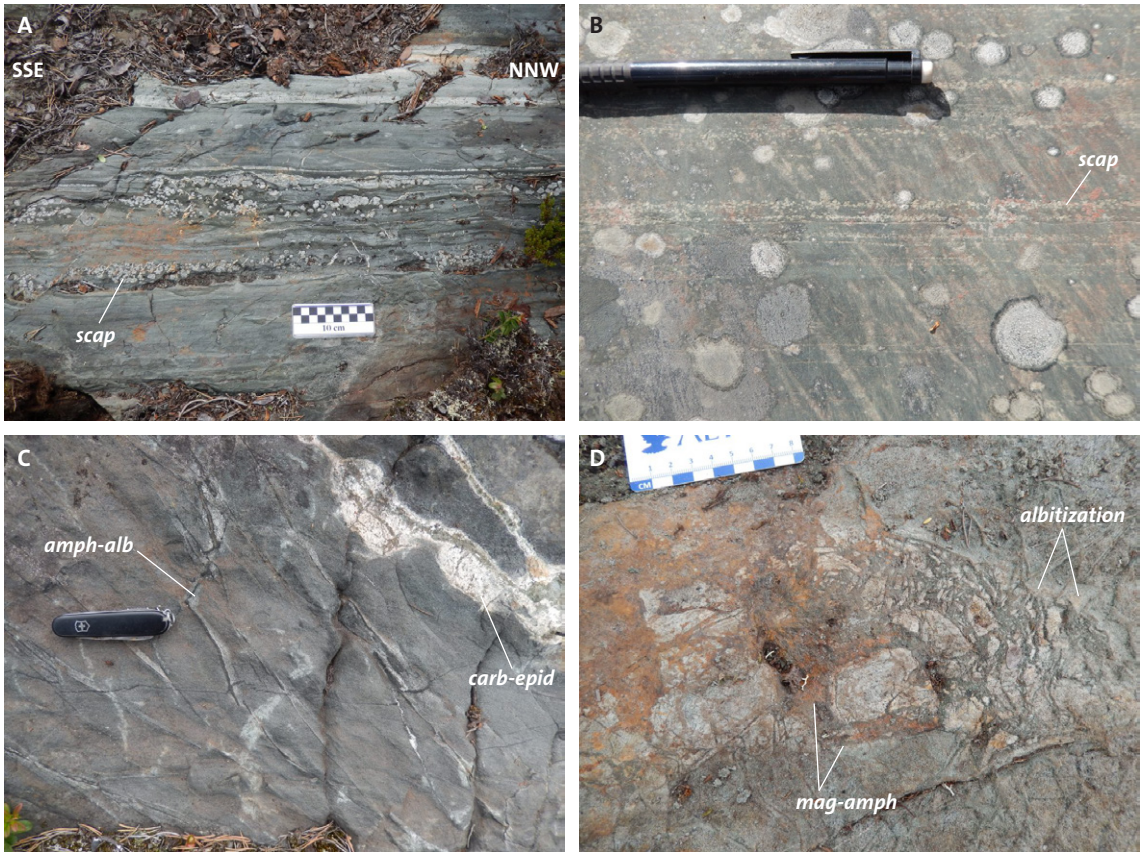

Figure 13. Alteration and mineralisation of laminated tuff. **A.** Banded, c. 0.5–1 cm large, creamy white scapolite porphyroblasts in laminated tuff (7523661/770545). **B.** Fine-grained (c. 0.1 cm) scapolite banding in laminated tuff (7524615/769180). **C.** Discordant actinolite±magnetite veinlets with albite halos cut by late-stage carbonate-epidote veining. The view is orthogonal to bedding. (7524028/769710). **D.** Brecciated and fractured tuff (adjacent to a metadolerite sill) consisting of albitised clasts in a magnetite-amphibole (actinolite?) matrix (7524013/769820).

more intensely albite altered when compared to the general scapolite-amphibole-altered host basalt appearance (e.g. Fig. 12a, e).

The basaltic tuffs at Nunasvaara (Upper greenstone formation) are also affected by alteration and veining (Fig. 13). In general, the alteration assemblage is similar to that seen in the lowermost basalts. An early, pervasive scapolite-actinolite-albite±magnetite assemblage typically occurs. Locally, relatively think (c. 3–10 cm) bands and zones of intense scapolite-amphibole±albite alteration are present containing scapolite porphyroblasts that are up to 1 cm in diameter (Fig. 13a). These bands are usually developed in tuff layers or beds with a more basaltic (mafic) composition. At other locations, scapolite banding is less intense and forms faint, thin (c. 0.1–0.5 cm), planar, sub-parallel seams (Fig. 13b).

Actnolite±magnetite veins also occur in the tuffs (Fig. 13c). These veins are typically 0.2–1 cm thick, planar to weakly wavy and locally display albite alteration halos. The veins do not have a preferred orientation. However, the majority of veins are sub-vertical and discordant to tuff bedding and laminae orientations.

At locations where doleritic sills intrude the tuff, the volcanic rock displays a more crystalline (hornfels) and altered appearance. At one location (7524013/769820) the rock is intensely albite-scapolite-amphibole altered and the alteration grades into a stockwork and breccia zone

containing blocky to irregular albitised volcanic clasts within a fine-grained magnetite-actinolite matrix (Fig. 13d).

Dolerite sills at Nunasvaara are also variably altered (Fig. 14). The pervasive alteration assemblage is similar to that affecting the basalts and tuffs. It is a fine- to medium-grained (c. 0.1–5 mm), moderate to intense scapolite-amphibole-albite-magnetite assemblage replacing primary pyroxene and plagioclase. On exposed surfaces the alteration imparts a speckled grey-white appearance to the rock (Fig. 10a–b). In the least altered outcrops, patchy fine-grained amphibole (actinolite?) and scapolite occur and can form irregular halos around disseminated pyrite grains. Albite clots and nodules are also seen (Fig. 14a). Magnetite is often associated with the pervasive actinolite and scapolite alteration and fine-grained scapolite-albite occurring in microfractures (Fig. 14b–c). This indicates that magnetite may have been remobilised during alteration. Where the dolerite is intensely altered, scapolite porphyroblasts within an amphibole-rich matrix replace the primary rock textures (Fig. 14d).

An example of an amphibole-rich, hydrothermal breccia was investigated at Nunasvaara (Fig. 15). A brief description of this occurrence is reported in Martinsson & Wanhainen (2000). The breccia is located at the contact between tholeiitic basalts and a relatively thick dolerite sill in the centre of the study area (7524795/772438). The exposed area is approximately 3 × 5 m and at its margins the breccia grades into an intensely scapolite-altered, intermediate intrusive rock with a somewhat dioritic appearance. About 300 m to the north-east, a scapolitised dio-

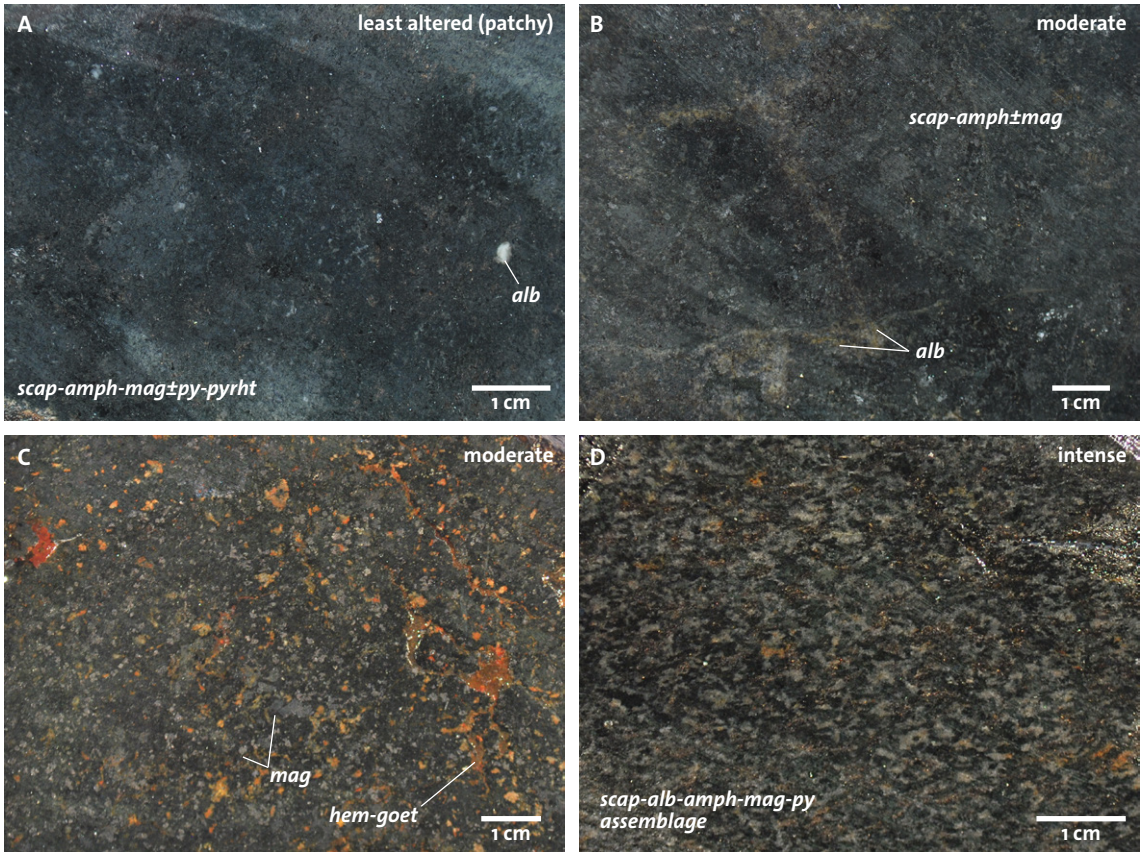

Figure 14. Dolerite alteration textures seen on wet slabs. All scale bars are 1 cm. **A.** Least altered (patchy) scapolite-amphibole (actinolite?)-magnetite assemblage with minor pyrite and pyrrhotite. **B–C.** Moderately developed, pervasive scapolite-amphibole-magnetite alteration. Albite halos associated with veinlets are also seen in C. **D.** Intense, pervasive scapolite-albite-amphibole alteration.

ritic intrusion also occurs (scapolite diorite of Martinsson & Wanhainen 2000). The breccia is matrix supported and contains irregular, blocky and angular, creamy white to pink clasts (c. 1–10 cm) within a fine- to medium-grained, dark greenish grey, amphibole-rich matrix (Fig. 15a). Amphibole net-veining that is texturally continuous with the matrix cross-cuts the clasts (Fig. 15b). The majority of clasts are intensely altered with a fine-grained powdery material (Fig. 15d). However, some clasts display a remnant granular texture suggesting derivation from an igneous rock (e.g. Fig. 15c).

Figure 16 shows the results of the preliminary mineralogical analysis of amphibole breccia using Raman spectroscopy on sample chip material. Spectrum 1 corresponds to the light coloured material in the clasts. The Raman spectrum of this material is diagnostic of albite. Spectrum 2 corresponds to the dark greenish grey material making up the matrix and the Raman spectrum of this material is diagnostic of actinolite. These data confirm the main mineralogical characteristics of the breccia. Further investigations on this type of breccia are ongoing, in particular the primary nature of the clasts.

Svecokarelian intrusive rocks at Nunasvaara

The Nunasvaara area is surrounded by a variety of Svecokarelian (c. 1.90–1.74 Ga) felsic and mafic intrusive rocks (Fig. 4). These include Haparanda-type gabbroid-dioritoid-granitoid bodies, broadly contemporaneous Perthite-monzonite-type gabbroid-granitoid plutons, and

Figure 15. Example of an amphibole-rich, matrix supported, hydrothermal breccia at Nunasvaara (7524795/772438). **A.** Breccia zone with angular, pale grey to white clasts in a dark greenish grey matrix. **B.** Clasts displaying net veining and banding that is texturally and mineralogically continuous with the matrix. **C–D.** Detailed view of breccia clasts displaying varying degrees of albitisation.

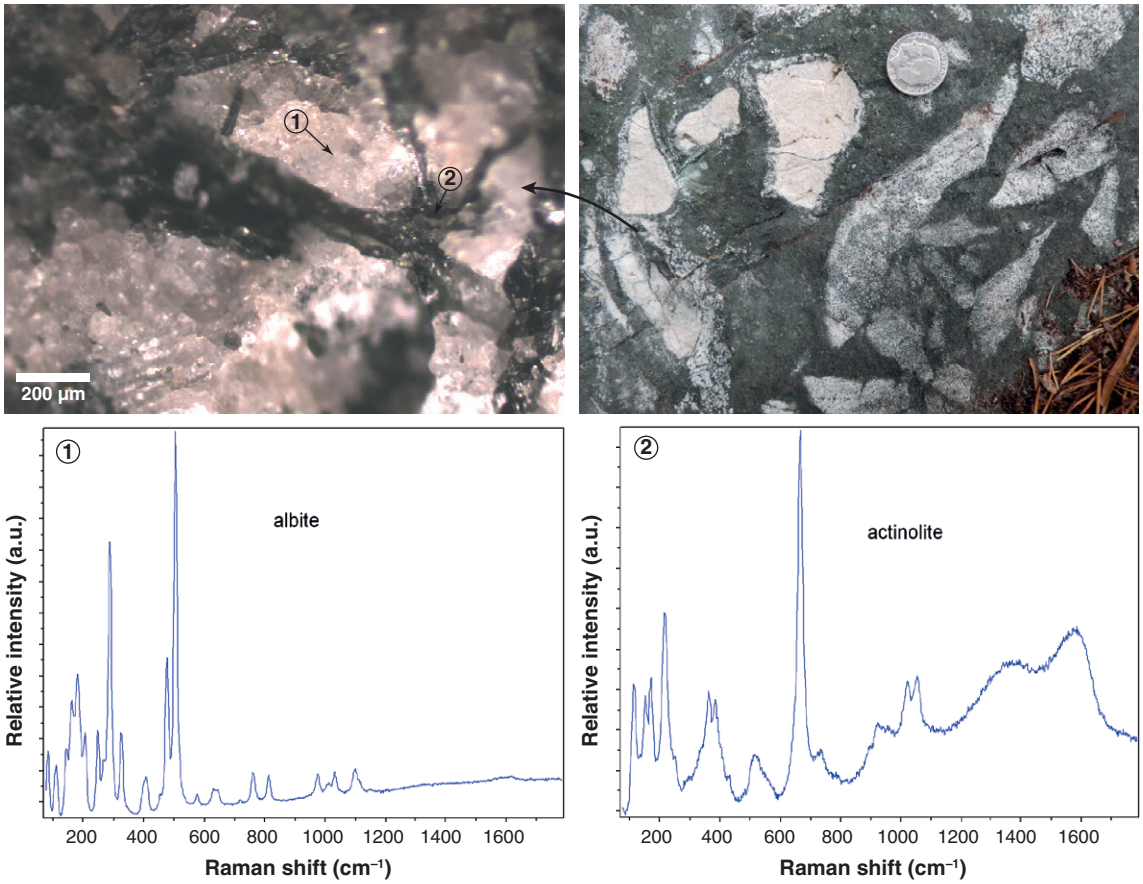

Figure 16. Mineralogical composition of Nunasvaara amphibole breccia shown in Fig. 15 using Raman spectroscopy of sample chips. Points 1 and 2 (upper left) are representative of the analysed material and provide diagnostic mineral spectra (bottom) corresponding to albite (clast material) and actinolite (matrix material), respectively. A.u. = arbitary units.

granite plutons (s.s.) belonging to the Granite-pegmatite suite. This latter suite represents the youngest phase of felsic magmatism in the region (e.g. Bergman et al. 2001).

At the western end of the sample profile (7525828/767462), a regionally extensive intermediate to felsic intrusion truncates the greenstone sequence (Figs. 3 and 4). Here, the rock is a medium grey to pinkish grey, medium- to coarse-grained (c. 3–10 mm), moderately to strongly foliated, amphibole-rich, intergranular quartz monzodiorite (Fig. 17a). Locally, it contains elongate mafic enclaves and patches that are generally aligned sub-parallel to the main foliation at c. 330/82 (Fig. 17b–c). The enclaves typically have diffuse margins and contain grains (xenocrysts) of felsic material similar to feldspar phenocrysts in the host monzodiorite (Fig. 17c). Locally, the quartz monzodiorite is cut by sub-vertical, mafic (doleritic?) dykes that are up to 1 m wide (Fig. 17b, d). These dykes are generally fine-grained and are typically orientated sub-parallel to the foliation (c. 310/82) in the quartz monzodiorite and the mafic enclaves (Fig. 17b–c). Rarely, the dolerite dykes contain elongate felsic enclaves and patches that resemble the host quartz monzodiorite (Fig. 17c).

The presence of doleritic dykes cross-cutting the larger quartz monzodiorite indicates that late-stage, mafic magmatism occurred in the area. However, since the quartz monzodiorite contains mafic enclaves that resemble the doleritic dykes and the dykes contain enclaves and xenocrysts that resemble the quartz monzodiorite, a phase of bimodal magmatism or magma

Figure 17. Felsic to intermediate intrusive rocks at Nunasvaara. **A.** Foliated, amphibole-bearing, quartz monzodiorite (7525823/767469). **B.** Doleritic dyke (c. 1 m) cross-cutting quartz monzonitoid with adjacent mafic enclaves (arrow) (7525823/767450). **C.** Close-up of B showing mafic enclaves aligned sub-parallel to the main mineral foliation and dyke contact. **D.** Dolerite dyke containing enclave material (arrow) similar to the wall rock quartz monzonitoid (7525823/767450).

mingling may have occurred, with material derived from each unit being entrained within the other during a protracted phase of magma emplacement.

Geophysical investigations of the greenstone sequence

The Nunasvaara area is covered in detail by both airborne and ground magnetic, gravity and electromagnetic (VLF) data (e.g. Figs. 18–20). Petrophysical information (rock density and magnetic susceptibility) also exists for most of the area. A summary of existing airborne and ground geophysical data covering the Nunasvaara area is available in Lynch & Jönberger (2013a).

The greenstone sequence generally has a low to moderate magnetic signature (Fig. 18). However, distinct high magnetic anomalies with curvilinear forms occur across the area. These anomalously high magnetic zones correspond to magnetite-bearing dolerite sills, skarn-type iron and sulphide mineralised horizons and magnetite-bearing alteration zones. Gabbroic intrusions (e.g. large ellipsoidal shape in the east corresponding to the Vittangi gabbro) generally have moderate magnetic signatures, while felsic intrusions in the south and west have reasonably homogeneous low magnetic signatures (Figs. 4 and 18).

On the gravity anomaly map (Fig. 19) the greenstone sequence corresponds to a pronounced gravity high (especially in the south-west), which indicates that the volcanic rocks probably continue at depth. Felsic intrusions correspond to gravity lows while gabbroic intrusions have a

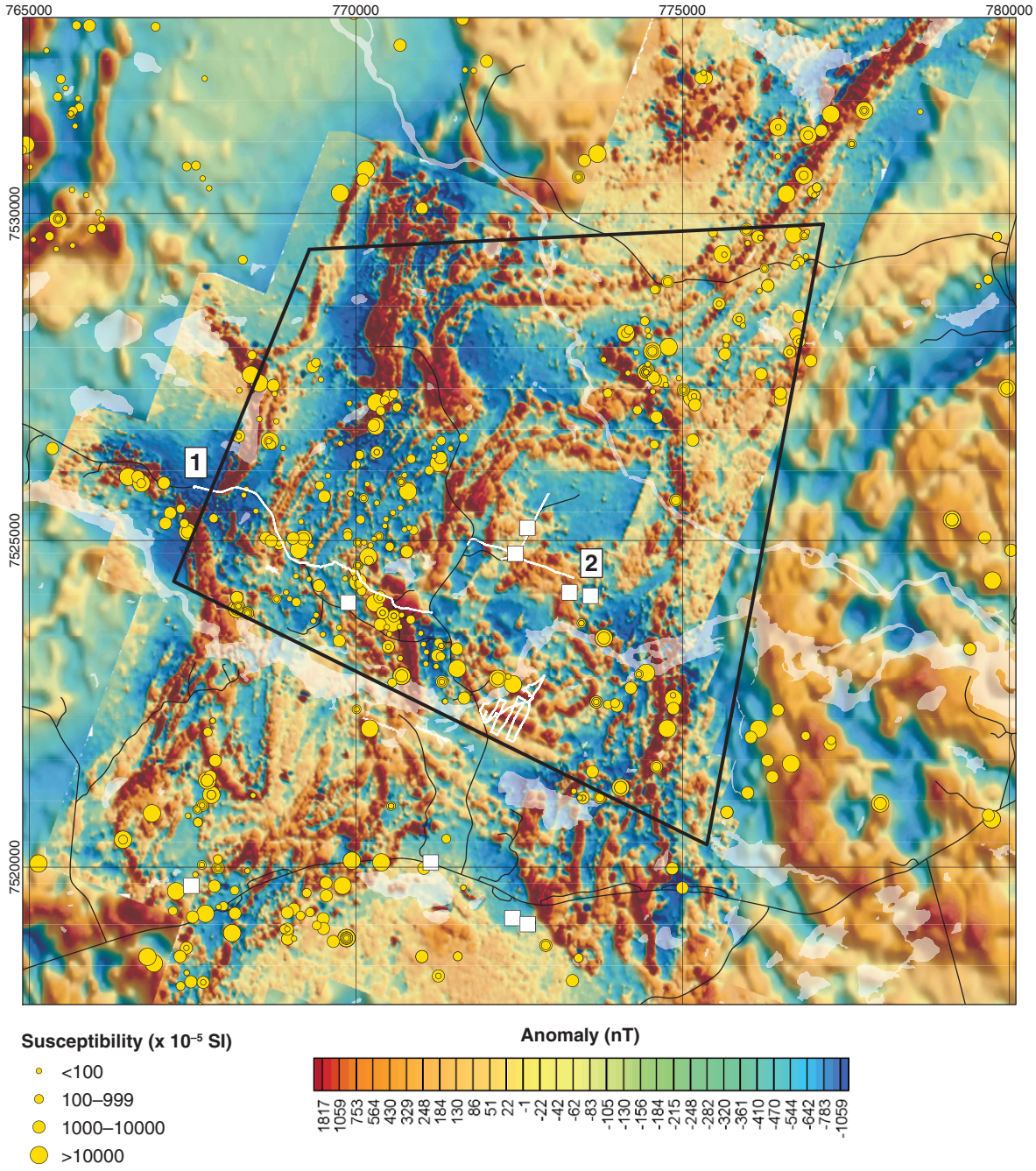

Figure 18. Combined airborne and ground magnetic anomaly map of Nunasvaara. Yellow circles represent (by proportional size) susceptibilities of historical petrophysical samples. The white lines represent ground measurements done in 2013 with geophysical profiles "1" and "2" labelled. White squares show the locations of spectrometry and petrophysical sampling.

moderate to high gravity signature (cf. Fig. 4 and Fig. 19). Two sub-circular gravity lows occur close to the centre of the study area which may indicate the presence of one or more buried felsic intrusions in this area (Fig. 19).

The electromagnetic map of the area (Fig. 20) shows distinctive curvilinear zones with high conductivity. These zones correspond to graphite-bearing schist horizons, skarn alteration zones containing sulphide mineralisation, and also lithological contact zones with relatively high per-

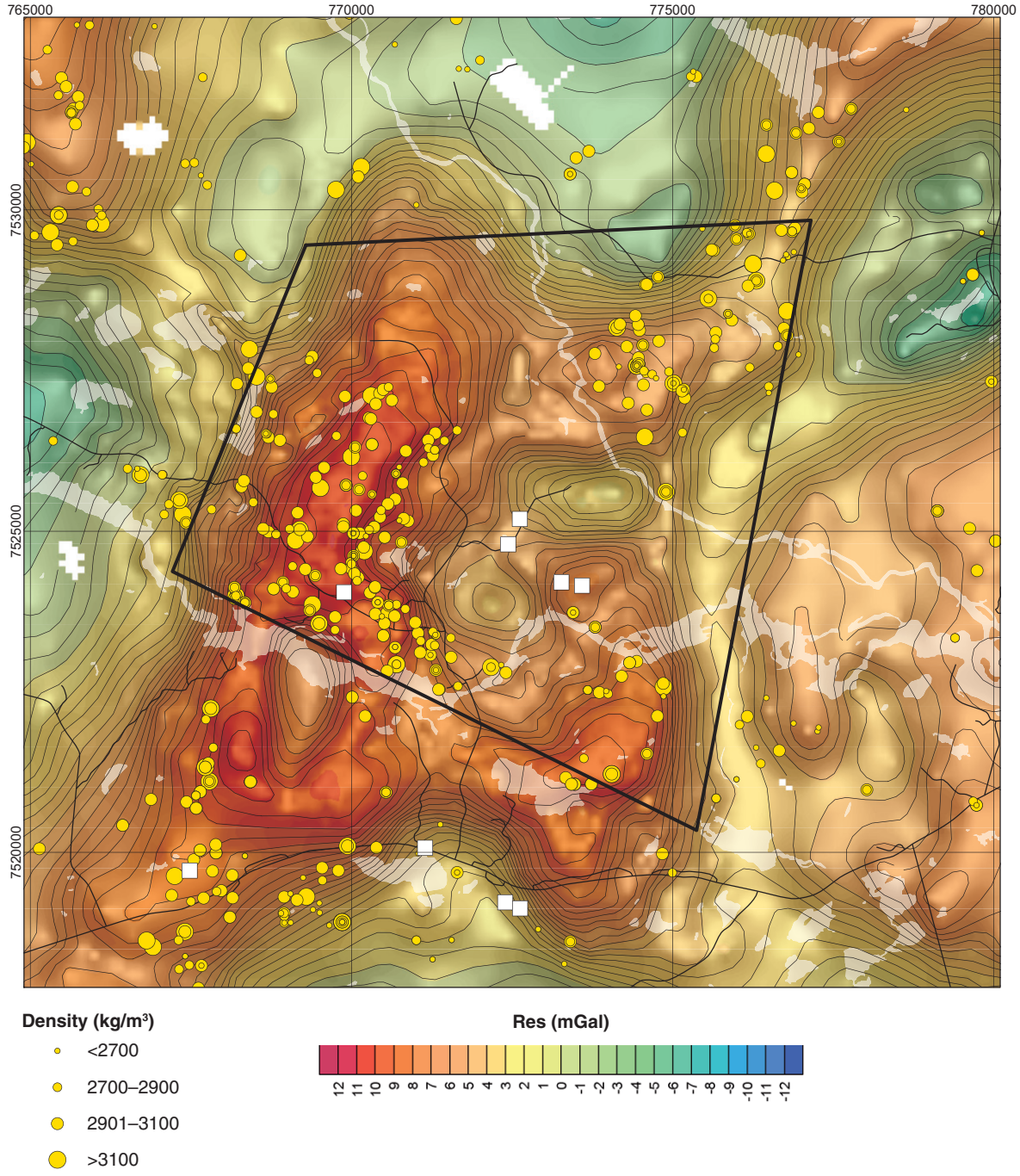

Figure 19. The gravity field at Nunasvaara. Yellow circles represent (by proportional size) historical petrophysical sample densities. White squares are 2013 gamma spectrometry and petrophysical sampling locations. The isoline interval is 0.5 mGal.

meability (e.g. doleritic sill contacts). In general, the greenstone pile (basalts and tuffs) has a relatively low to moderate electrical conductivity signature.

Geophysical field work in 2013 was carried out over five days with the aim of correlating and modelling the greenstone stratigraphy based on its magnetic and electromagnetic properties. Measurements were made along two linear profiles (labeled 1 and 2 in Fig. 18) using ground magnetometer and VLF instruments. These profiles broadly correspond to the bedrock observa-

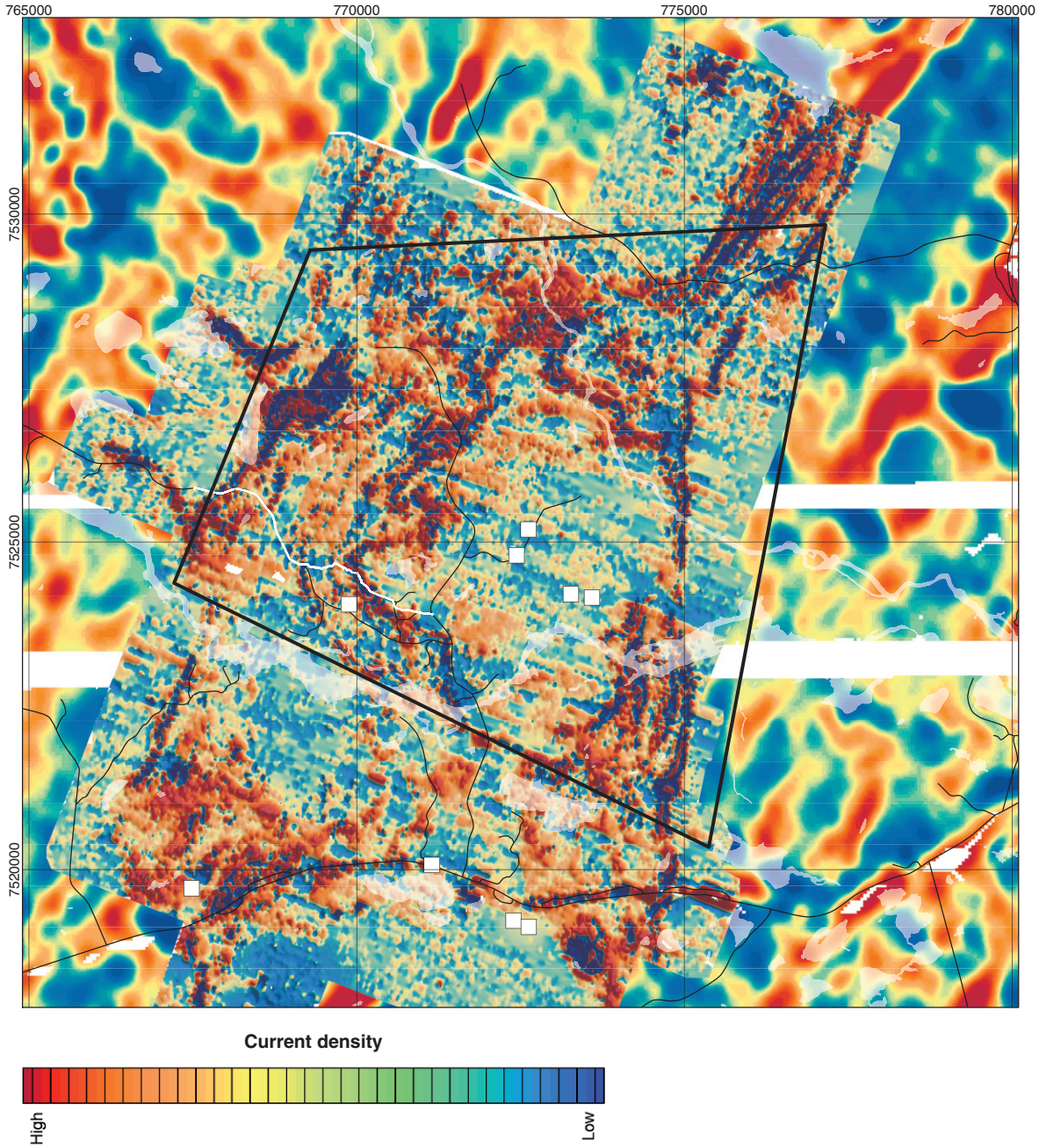

Figure 20. Electromagnetic map of Nunasvaara. The more spatially coarse areas (at the map margins) represent current densities derived from airborne VLF data (red indicates good conductivity). The detailed high resolution data (map centre) shows ground slingram measurements (blue represents good conductivity). White line shows 2013 ground VLF measurement corresponding to profile 1 in Figures 18 and 22. White squares represent 2013 gamma spectrometry and petrophysical sampling locations.

tion and sampling points shown in Figure 3. An additional ground magnetometer survey was conducted at the southern border of the Nunasvaara area (Fig. 18).

Figures 21–23 show the results of the magnetometer and VLF measurements made along geophysical profiles 1 and 2. The variation in the magnetic field along profile 1 (Fig. 21) shows anomalous magnetic peaks over the skarn-type alteration and mineralisation zone in the northwest (c. 800 m profile segment), and a relatively thick, scapolite altered, magnetite-bearing dol-

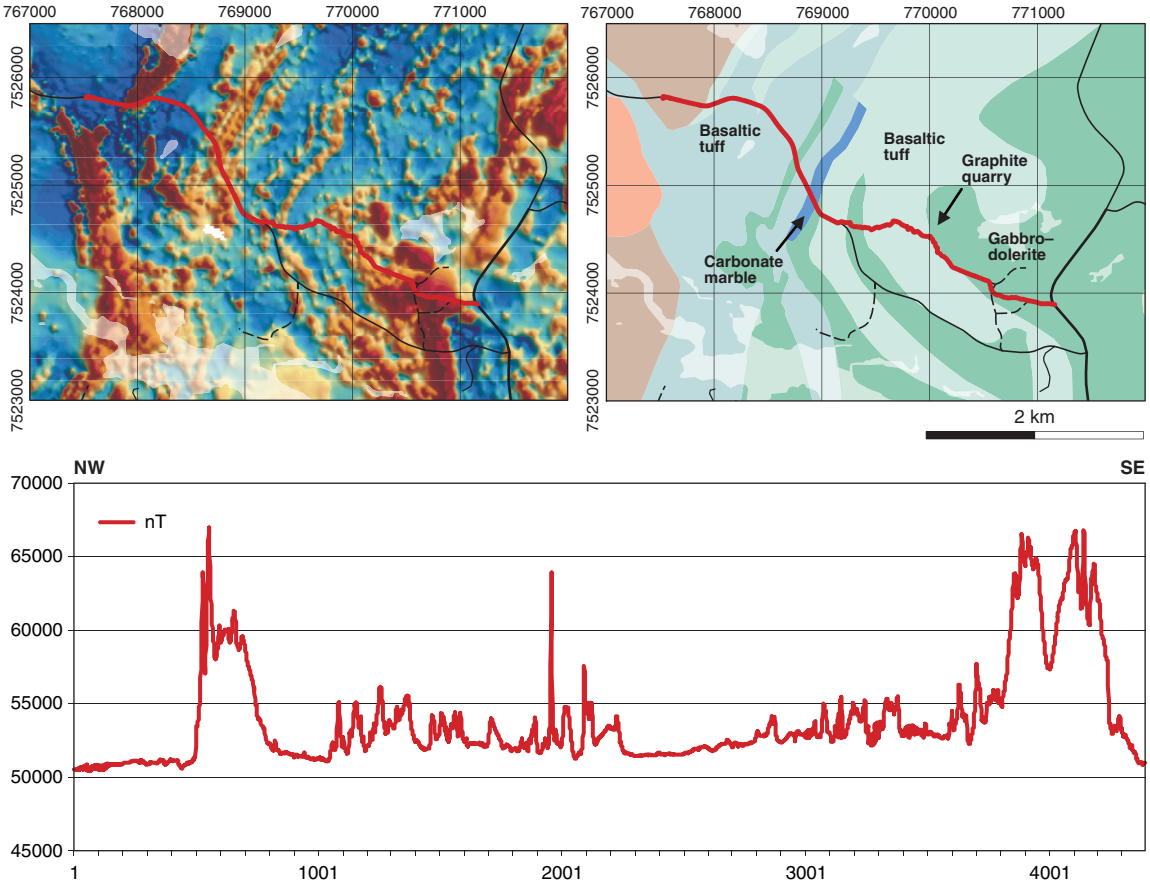

Figure 21. Geophysical profile 1 in the western Nunasvaara area (see Fig. 18). The plotted graph shows the variation in the magnetic field along the profile.

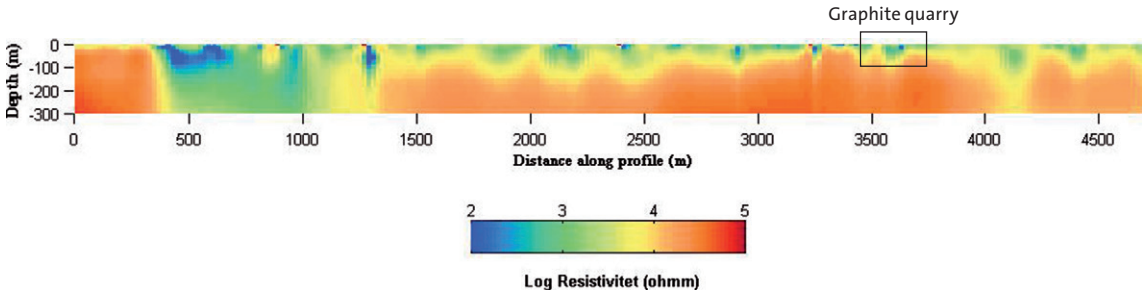

Figure 22. Inversion model of the VLF measurements made along geophysical profile 1.

eritic sill in the south-east (c. 4000 m segment). A relatively narrow, high magnetic peak is also seen in the middle of profile 1. This may correlate with the stratigraphic position of a banded ironstone (c. 1975 m profile segment). Between these prominent magnetic peaks, the greenstone sequence (basaltic tuffs and intercalated metasedimentary rocks) generally have a low magnetic signature, although some variation exists that may reflect local magnetite-bearing alteration and the occurrence of narrower, magnetite-bearing doleritic sills.

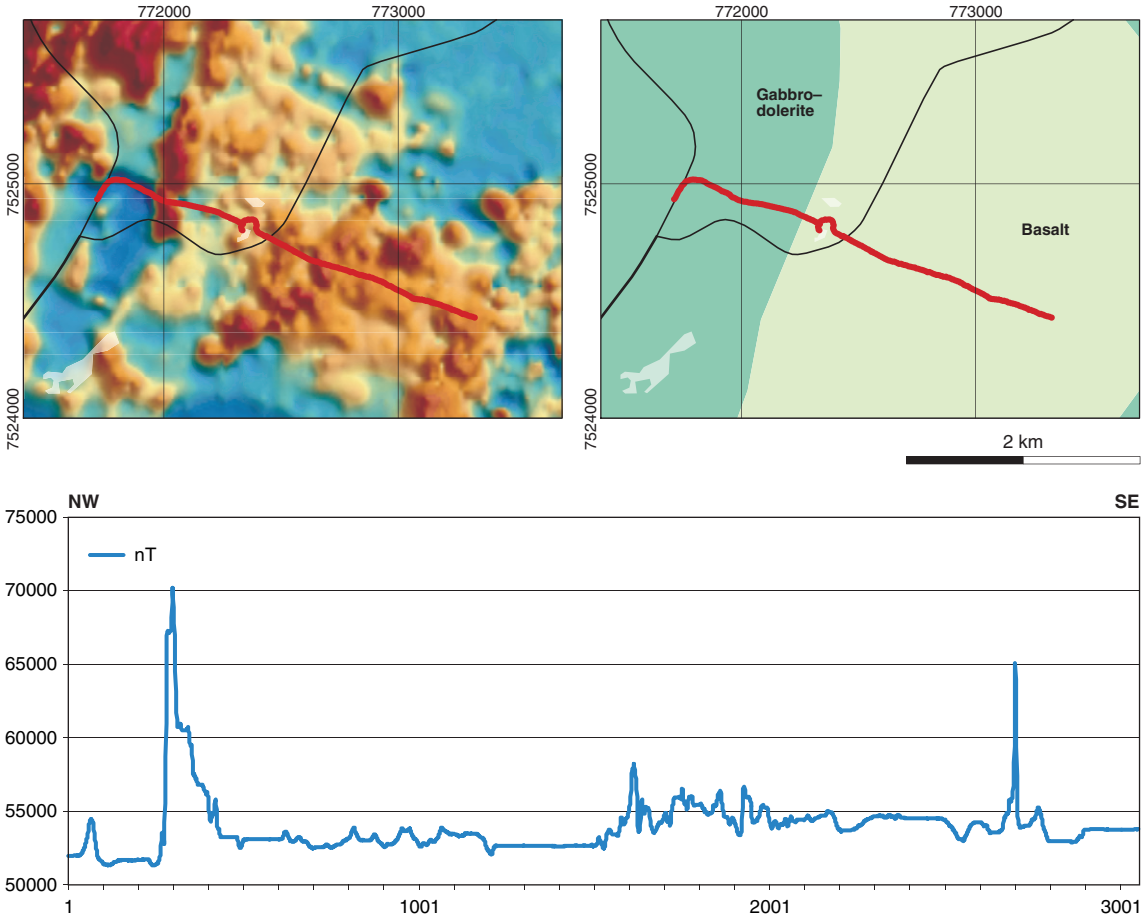

Figure 23. Geophysical profile 2 in the central Nunasvaara area (see Fig. 18). The plotted graph shows the variation in the magnetic field along the profile.

Figure 22 shows the result of an inversion model of the VLF data measured along profile 1. The most conductive area (blue-green) can be seen in the western end of the profile (c. 400–1000 m segment) corresponding to an area with skarn-type alteration and related sulphide mineralisation. The position of the graphite quarry at Nunasvaara is also highlighted on the profile.

Figure 23 shows the result of the magnetometer measurements along geophysical profile 2 (Fig. 18). The data display a strong, positive magnetic anomaly in the western part of the profile (c. 350 m segment) which correlates with a linear magnetic zone seen on the magnetic map. This anomaly probably corresponds to a magnetite-bearing dolerite. Another highly magnetised peak occurs in the eastern part of the profile (c. 2800 m segment). This area contains tholeiitic basalts of the Lower greenstone formation that are affected by scapolite-amphibole-magnetite alteration and magnetite-bearing veining (e.g. Fig. 12). Between these prominent magnetic peaks, the greenstone sequence (tholeiitic basalts, dolerite) generally has a low magnetic signature, although some minor variation exists within the basalt unit reflecting localized magnetite-bearing alteration effects.

Additional geophysical work at Nunasvaara included gamma spectrometer measurements and the collection of petrophysical samples (Fig. 24). Airborne uranium data for the area generally shows low uranium concentrations (c. 0.3–4 ppm) across the greenstone pile. Spectrometer measurements on Lower greenstone group basalts in the centre of the key area returned average concentrations of 0.5% potassium, 0.4 ppm uranium and 0.4 ppm thorium (n=4). Basaltic

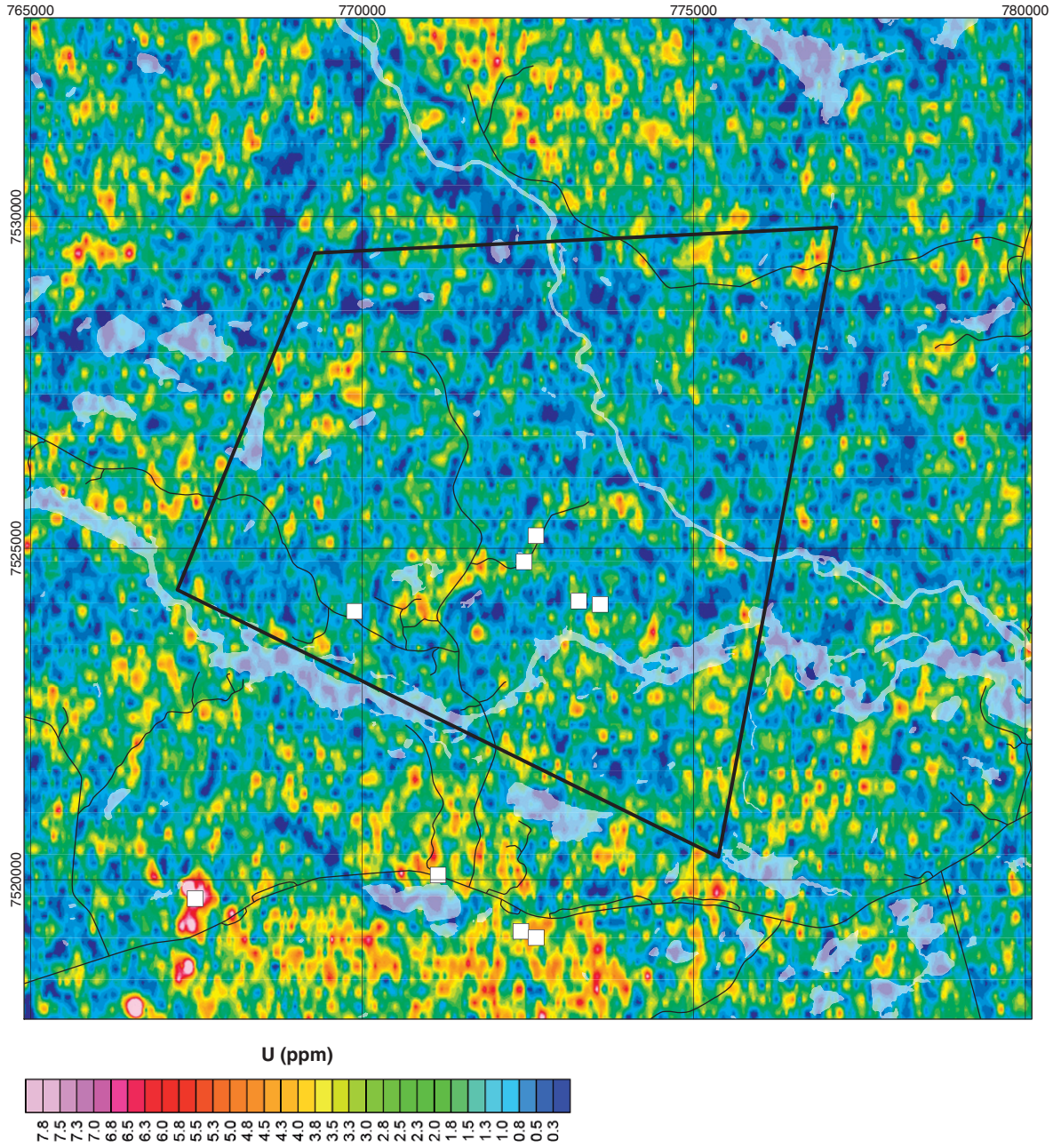

Figure 24. Airborne uranium anomaly map of Nunasvaara. White squares represent 2013 gamma spectrometry and petrophysical sampling locations.

tuffs (Upper greenstone formation) further to the west (7524051/769884) returned average concentrations of 0.1% potassium, 0.0 ppm uranium and 0.3 ppm thorium (n=2), while measurement of a scapolitised dioritic intrusion, close to the amphibole breccia previously described (7525191/772623), gave average concentrations of 0.2% potassium, 0.7 ppm uranium and 7.0 ppm thorium (n=3).

Higher uranium concentrations (c. 3–10 ppm) occur to the south of the key area, coincident with several granitic intrusions and known uranium mineralisation (Fig. 24). Spectrometer measurements on granite outcrops close to route E45 gave average concentrations of 4.0% potassium, 3 ppm uranium and 22 ppm thorium (n=9). Further to the west (7519717/767484),

coincident with an airborne-derived high uranium anomaly, granite and rhyolite is well exposed. Here, granitic bedrock returned average concentrations of 3.9 % potassium, 27 ppm uranium and 21 ppm thorium, while concentrations in the rhyolite were 6.0% potassium, 12 ppm uranium and 11 ppm thorium. Locally, the granite in this area has uranium concentrations up to 84 ppm which confirms the anomalous nature of the area.

FIELD ACTIVITIES IN THE SAARIJÄRVI AREA

The Saarijärvi key area (SKA) is located approximately 15 km south-west of Kiruna (Figs. 1 and 25). The bedrock geology of the area has been described in earlier SGU reports and maps by Geijer (1931), Ödman (1957) and Offerberg (1967). Three 1:50 000-scale bedrock maps from SGUs Af map series cover the area and represent the most detailed mapping. These are 29J Kiruna NV (Af 1), 29J Kiruna NO (Af 3) and 29J Kiruna SO (Af 4, Offerberg 1967, Offerberg & Nilsson 1967). A compilation of the area's bedrock mapping, geochronology, geochemistry and geophysical data is presented in Lynch & Jönberger (2013b).

The Saarijärvi key area is centered on a package of volcanic rocks which incorporate parts of the Kiruna greenstone group and overlying Porphyry group volcanic rocks. Minor metasedimentary horizons also occur within the various volcanic sequences (e.g. Kurravaara conglomerate, Kumpulainen 2000). Intrusive rocks in the area consist of variably metamorphosed syenitoids and gabbroids belonging to the Perthite monzonite suite (e.g. Witschard 1984). A small syenitoid stock, assigned to the Archean, occurs in the southern part of the area (Skiöld & Page 1998). Minor doleritic, granitic and syenitic dykes and veins are also known. The area hosts iron and copper-gold mineralisation, including the Pahtohavare and Rakkurijärvi deposits (e.g. Lindblom et al. 1996, Smith et al. 2007), while the broader region is considered to be prospective for IOCG-type mineralisation (e.g. Carlon 2000).

2013 bedrock observations, structural measurements, bedrock sampling and ground geophysics were conducted mostly in the southern and eastern parts of the key area (Fig. 25 and 31). The aims of the field work were: (1) to investigate Archean and Svecofennian syenitoid plutons in the southern Saarijärvi key area, along with other intrusive (granitoid) rocks, (2) to investigate a north-east trending deformation zone within Porphyry group volcanic rocks at the eastern end of the Saarijärvi key area, to understand links between deformation, alteration and mineralisation, (3) to sample a conglomeratic unit in the western Saarijärvi key area for detrital zircon studies, and (4) to conduct ground magnetic measurements (along with reconnaissance petrophysical sampling) in two areas in the southern key area which would complement aims 1 and 2.

Archean and Svecokarelian plutonism

In the south-central Saarijärvi key area (Jänkänalusta), an oblate, north-east orientated syenitoid pluton (c. 2 x 5 km) intrudes volcanic rocks of the Kiruna greenstone group and Porphyry group (Fig. 25). This pluton, presently assigned to the Svecokarelian granite-syenitoid-gabbroid association (Offerberg 1967, Bergman et al. 2000), was investigated in order to characterise Svecofennian syenitoid magmatism in the Kiruna area and potential links between felsic magmatism, alteration and (epigenetic) mineralisation. The studied intrusion also represents the most western example of a syenitoid pluton in northern Norrbotten (cf. Bergman et al. 2000).

The majority of existing mapped outcrops occur within the northeastern part of the intrusion (Fig. 25). These outcrops were visited and sampled for further mineralogical, geochemical and geochronological studies. The rock is typically a reddish pink, medium- to coarse-grained (0.2–1.2 cm), massive to locally foliated, K-feldspar-rich quartz alkali syenite that displays moderate to intense, pervasive potassic alteration (Fig. 26). Essential mineralogy is quartz (c. 5–10 vol.%),

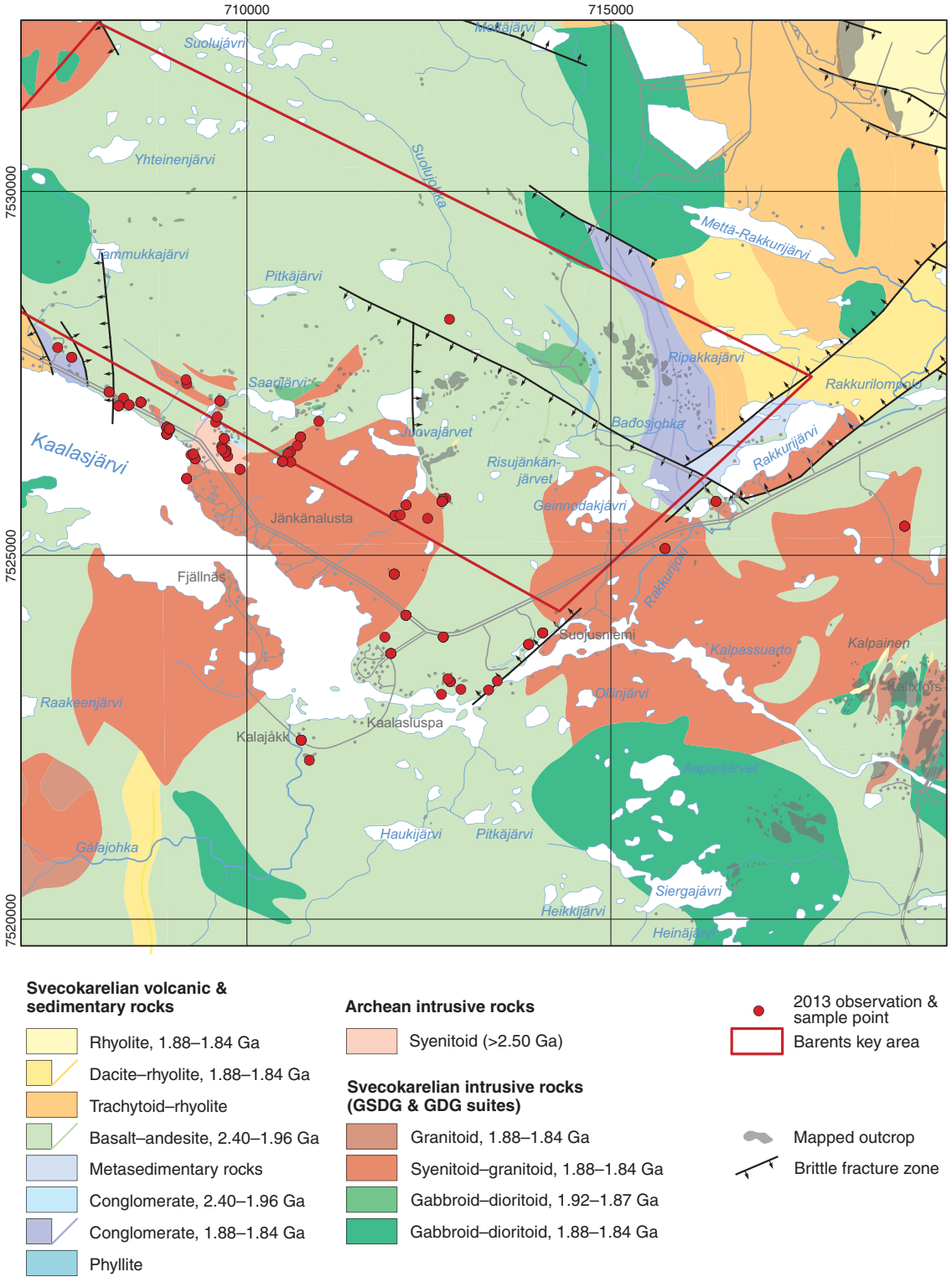

Figure 25. Bedrock geology of the Saarijärvi area based on SGU's local scale (1:50 000) database showing 2013 bedrock observation and sampling locations.

plagioclase feldspar (5–10%), alkali feldspar (50–60%), amphibole and possible biotite (10–15%). Mafic minerals have a dull greenish appearance suggesting chloritisation or sercitisation.

Reddish-pink, fine grained, K-feldspar occurs as a pervasive alteration that affects the majority of the syenite outcrops (e.g. Fig. 26a, d). K-feldspar staining is commonly seen replacing plagioclase and albite. Locally, thin, dark grey amphibole-biotite net veining of alkali feldspar phenocrysts is also seen. This may be part of the potassic assemblage. Rare pyrite is associated with the black alteration material replacing feldspar. Secondary anatase overprints amphibole. Secondary patchy hematite-goethite is also seen. Locally, thin, discontinuous, generally barren quartz veinlets and apparent tension gashes occur (Fig. 26b).

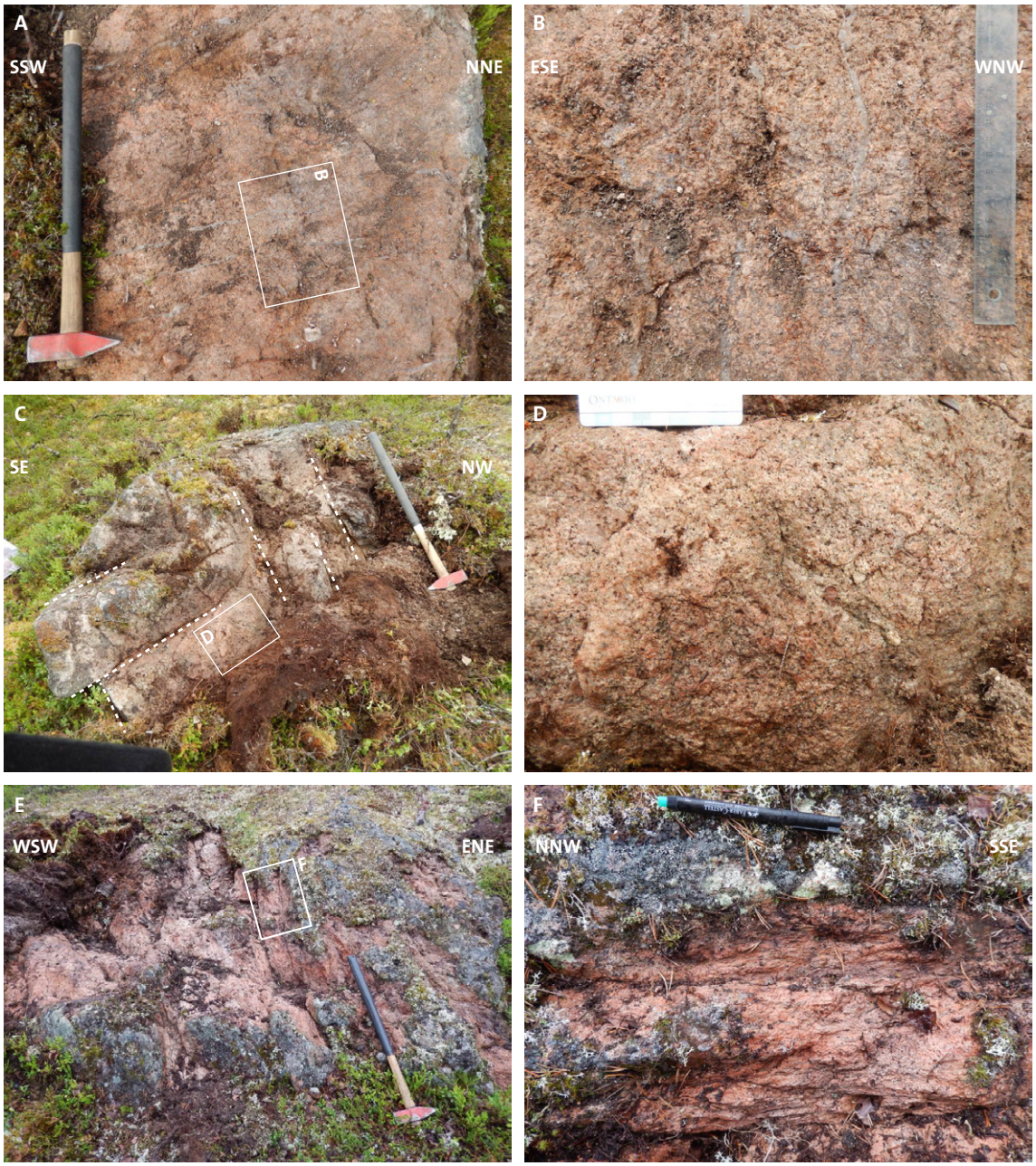

Figure 26. Quartz alkali syenite at Saarijärvi. **A–B.** Example of reddish-pink, orthoclase-rich quartz syenitoid. Barren quartz veins are also seen (7526625/710733). **C–D.** Example of reddish-pink, orthoclase-rich syenitoid outcrop with several joint sets (7526290/710488). **E–F.** Example of a quartz syenitoid outcrop with a more deformed, brittle fabric developed (7524744/712021).

The alkali syenite is generally massive. However, locally it contains a relatively strong, brittle, planar fabric (Fig. 26e–f). This fabric imparts a foliated appearance which has a general north-west to south-east orientation and is sub-vertical. All syenite outcrops generally contain two sub-vertical joint sets along with sub-horizontal jointing where exposed (Fig. 26c).

The contact between the syenite intrusion and the host volcanic rocks along its northern, eastern and western margins is generally sharp and discordant (cf. magnetic map in Fig. 31). At one location on the north-east shore of Lake Kaalasjärvi (7526055/709171), the contact between host greenstone basalts and the quartz alkali syenite is seen. Here, a planar, penetrative foliation in the volcanic rocks is sub-parallel to the intrusive contact.

Measured magnetic susceptibility values from syenite outcrops range from 7 to $4\,030 \times 10^{-5}$ SI, with an average value of 565×10^{-5} SI (n=112). The relatively narrow range in susceptibility values, along with a relatively low average, is a likely consequence of the generally felsic nature of the pluton, low magnetite abundances and the effects of the overprinting potassic alteration.

On the north-west margin of the previously described syenite intrusion (c. 1 km south-west of Lake Saarijärvi), a small (c. 400 × 800m) Archean syenitoid stock occurs (Fig. 25, Offerberg 1967). This intrusion represents the southernmost exposure of Archean basement in the Kiruna area. Observations and sampling of the stock were conducted to better constrain its geologic and geochemical characteristics.

The rocks is a reddish pink, medium- to coarse-grained (c. 0.1–1 cm), foliated to locally massive, K-feldspar-rich quartz syenitoid (Fig. 28). The essential mineralogy is quartz

Figure 27. Contact (dashed line) between quartz alkali syenite and foliated basalt at Lake Kaalasjärvi (7526055/709171). Foliation in the basalt is sub-parallel to the contact.

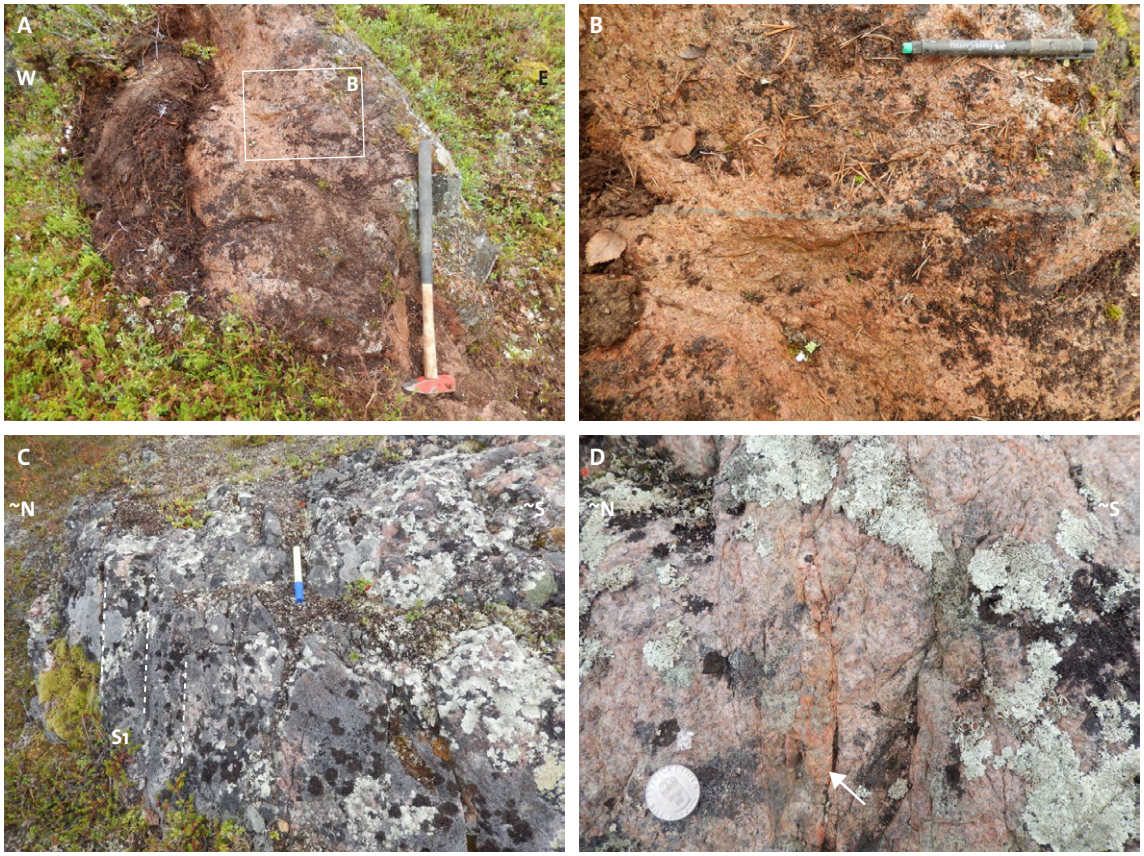

Figure 28. Archean syenitoid rocks at Saarijarvi. **A–B.** Example of reddish-pink, orthoclase-rich (altered?) pluton with local barren quartz vening and quartz-filled tension gashes (7526416/709696). **C.** Archean syenitoid containing a strongly developed spaced cleavage (S1, 7526605/709685). **D.** Closer view of brittle foliation and example of potassic alteration adjacent to a fracture plane (arrow, 7526605/709685).

(c. 8–10 vol.%), plagioclase feldspar (3–5%), alkali feldspar (50–60%) and amphibole (5–7%). Mafic minerals have a low abundance and are chloritised or sericitised with a greenish grey appearance. Pervasive potassic alteration consisting of reddish-pink, fine-grained, hydrothermal K-feldspar (overprinting plagioclase and albite) affects the rock (Fig. 28a–b). Secondary anatase occurs after amphibole or titanite, along with patchy hematite-goethite staining. Locally, the rock contains chlorite- and sericite-rich zones representing more intense zones of alteration and perhaps more localised deformation. Less than 1 cm thick, planar to weakly wavy, barren quartz veinlets and tension gashes occur with typically west to west-north-west orientations (Fig. 28b). These veinlets are similar in appearance to quartz veinlets seen in the neighbouring quartz alkali syenite pluton previously noted.

The quartz syenitoid is generally foliated, although more massive areas also occur. The foliation is a penetrative, spaced cleavage (Fig. 28c–d). It is typically west-north-west orientated and sub-vertical. In some locations, locally intense potassic alteration is developed along cleavage planes and fracture surfaces (Fig. 28d).

Measured magnetic susceptibility values from the Archean syenitoid ranged from 9 to $3\,830 \times 10^{-5}$ SI, with an average value of 375×10^{-5} SI (n=56). The relatively narrow range in susceptibility values, along with a relatively low average, is a likely consequence of the general felsic nature of the stock, low mafic mineral abundances and the effects of overprinting potassic alteration.

Figure 29. Deformed volcanic rocks at Saarijärvi containing mylonitic fabrics and kinematic indicators. **A–B.** Dominant, penetrative, sub-vertical foliation planes (S1) with aligned feldspar phenocrysts and rotated porphyroclasts indicating eastern side up kinematics (7524176/712181). **C–D.** The same S1 penetrative foliation as in A and B, producing S-C type fabrics and delta porphyroclasts indicating an "eastern side down" shear-sense (7523877/712695).

At the ourcrop scale, the Archean stock bears a petrological resemblance to the larger Svecokarelian alkali syenitoid pluton to the east. Both intrusions have similar mineralogical, textural and alteration characteristics. However, the Archean stock appears to be locally more intensely deformed. Further mineralogical and geochemical investigations will help resolve the geologic variation between the two intrusive units.

Volcanic rocks at Kaalasluspa: a link between deformation, alteration and mineralisation?

In the Kaalasluspa area of Saarijärvi, deformed porphyritic volcanic rocks (assigned to the Porphyry group) crop out to the east of the Svecokarelian quartz alkali syenite pluton previously described (Figs. 29–30). This area represents the south-west extension of a regional-scale deformation zone that trends south-west from Lake Rakkurijärvi and hosts known IOCG-style mineralisation (e.g. Rakkurijärvi iron deposit, Smith et al. 2007, 2010). The volcanic rocks were investigated to understand deformation processes in the area and test the links between localised high strain zones and variably developed alteration and mineralisation.

The porphyritic rocks contain a moderate to intense, penetrative, planar foliation (designated S1, Fig. 29a, c). Locally, the foliation forms high strain zones displaying mylonitic fabrics (Fig. 29b, d). Feldspar phenocrysts have a stretched to elongate shape and are preferentially

aligned parallel to S1 planes (Fig. 29b). At one location (7524176/712181), rotated feldspar porphyroclasts indicate an east-side-up sense of movement (Fig. 29b). Directly to the east-south-east (7523877/712695), S-C fabrics and delta porphyroclasts suggest east-side-down kinematics and related transtensional deformation (Fig. 29d). At this location, the rock displays a moderate to intense alteration consisting of reddish-pink staining of feldspar phenocrysts in a dark grey, amphibole-magnetite matrix (Fig. 29d).

The preliminary results of orientation measurements made on S1 foliation planes at Kaalasluspa are presented in Figure 30. In the east (closest to a mapped fault and within the Rakkurijärvi deformation zone) foliation planes strike north-east–south-west, are sub-vertical, and generally sub-parallel to the orientation of the Rakkurijärvi deformation zone. In the west (closer to the quartz alkali syenite intrusion), S1 planes have a more north-north-east to north–south orientation and appear less influenced by the effects of the deformation zone. The variation in S1 orientations from north-east to north-north-east and north may also reflect the influence of the intrusive contact between the syenite pluton and the host volcanic rocks (cf. Bergman et al. 1993).

The deformed volcanic rocks at Kaalasluspa also display the effects of variably developed potassic alteration (hydrothermal orthoclase±actinolite±biotite±magnetite; cf. Fig. 29d). A moderate to intense, pervasive alteration occurs in the eastern part of the area, close to a mapped fault and within the Rakkurijärvi deformation zone (Fig. 30). Further to the west (adjacent to the alkali syenite pluton), potassic alteration is less pervasive and occurs as stringer-type veins, patches affecting volcanic phenocrysts and linear zones. Thin aplitic veins with a somewhat syenitic (K-feldspar-rich) composition also occur in this area.

Ground magnetic measurements of volcanic and plutonic rocks at Saarijärvi

The Saarijärvi area is extensively covered by airborne and ground magnetic, gravity and electromagnetic (VLF) data (Figs. 31, 34 and 35). Petrophysical information (rock density and magnetic susceptibility) primarily exists for localities in the south and east, coincident with known mineralisation and access infrastructure (Figs. 31 and 34). A summary of the existing airborne and ground geophysical datasets is provided in Lynch & Jönberger (2013b).

During 2013, two new magnetometer surveys were conducted in the southern part of the key area (survey areas highlighted in Fig. 31). Reconnaissance-level gamma spectrometer measurements and petrophysical sampling were also conducted. The aims of the magnetic measurements were: (1) to investigate the magnetic properties of deformed volcanic rocks in the Kaalasluspa area (Fig. 32), and (2) to measure the magnetic signature of the Archean syenitoid stock near Lake Saarijärvi (7526499/709597) and map its contact relationships with adjacent greenstones and the larger syenitoid pluton to the south (Fig. 33).

Figure 32 shows the results of the ground magnetometer survey of the deformed volcanic rocks at Kaalasluspa. Inferred structural lineaments and linear zones of deformation are also plotted. The area corresponds to the map area shown in Figure 30 containing orientation data of foliation planes within deformed and altered volcanic rocks. In the centre of the area, the lineaments have a predominant north-north-east orientation. In the north of the area, the lineaments deflect toward a more north–south orientation. This deflection appears to follow the contact of the syenitoid intrusion to the west (strong magnetic low area in Fig. 32). The magnetic data in the south-east indicates more of a north-east alignment, coincident with the orientation of the Rakkurijärvi deformation zone and a prominent, regional-scale electromagnetic conductor seen in the airborne VLF data (Fig. 35). Overall, there appears to be a general correspondence between lineament features derived from the ground magnetic data (Fig. 32) and the orientation of deformation fabrics seen in the volcanic rocks (see Fig. 30).

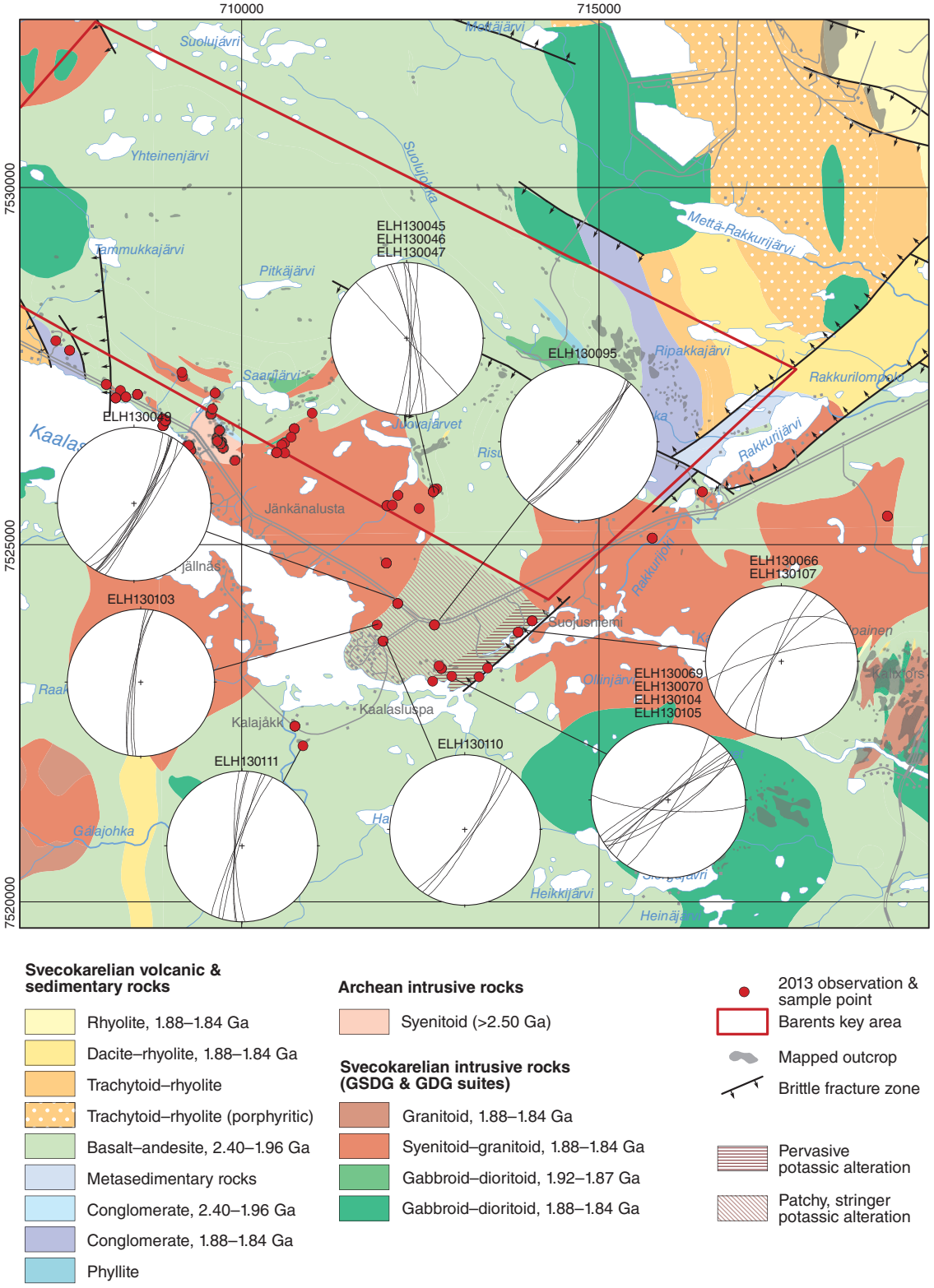

Figure 30. Orientation measurements of sub-vertical, penetrative foliation planes (S1) developed in volcanic rocks in the Kaalasluspa area, south-eastern Saarijärvi area (as shown in Fig. 20). Zones of potassic alteration (fine-grained, pervasive to patchy, reddish-pink orthoclase) affecting the volcanic rocks are also shown.

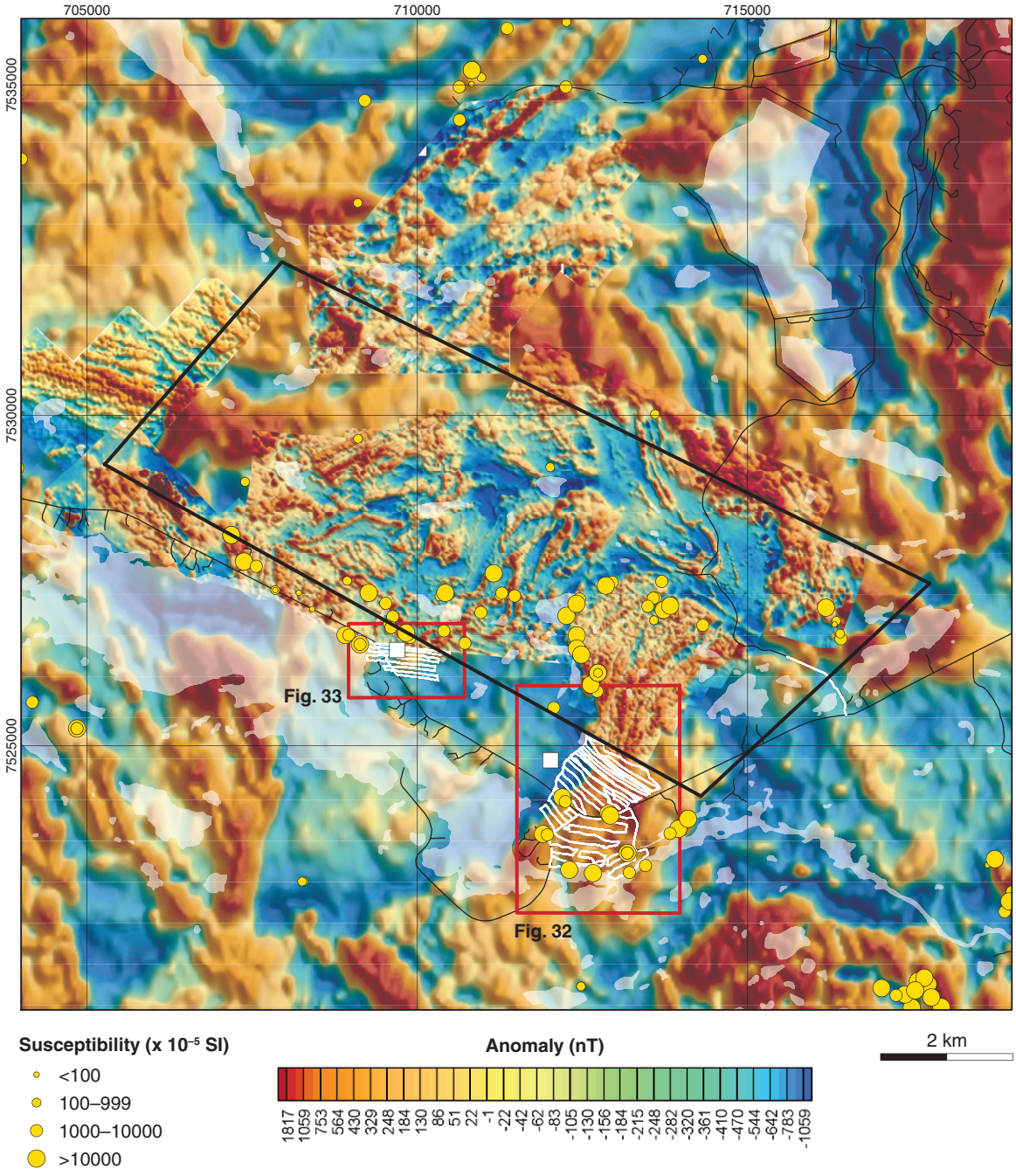

Figure 31. Combined airborne and ground magnetic anomaly map for the Saarijärvi area. Yellow circles represent (by proportional size) magnetic susceptibilities of historical petrophysical samples. White lines are 2013 ground magnetic measurements shown in Figs. 32–33. White squares show 2013 gamma spectrometer and petrophysical sample locations.

Figure 33 shows the results of the ground magnetometer survey conducted over the Archean syenitoid stock near Lake Saarijärvi (cf. Fig. 31). The magnetic data has a somewhat heterogeneous appearance and displays several discontinuous low anomalies surrounding a central magnetic high zone. A data mismatch between historical ground magnetic data (at top) and the new 2013 data (centre) is also seen. The sub-circular magnetic high in the centre of the survey area is preliminarily interpreted to reflect basalts of the Kiruna greenstone group. The contact with the Archean stock is not sharp and may reflect deformation in the area. Further interpretation is ongoing.

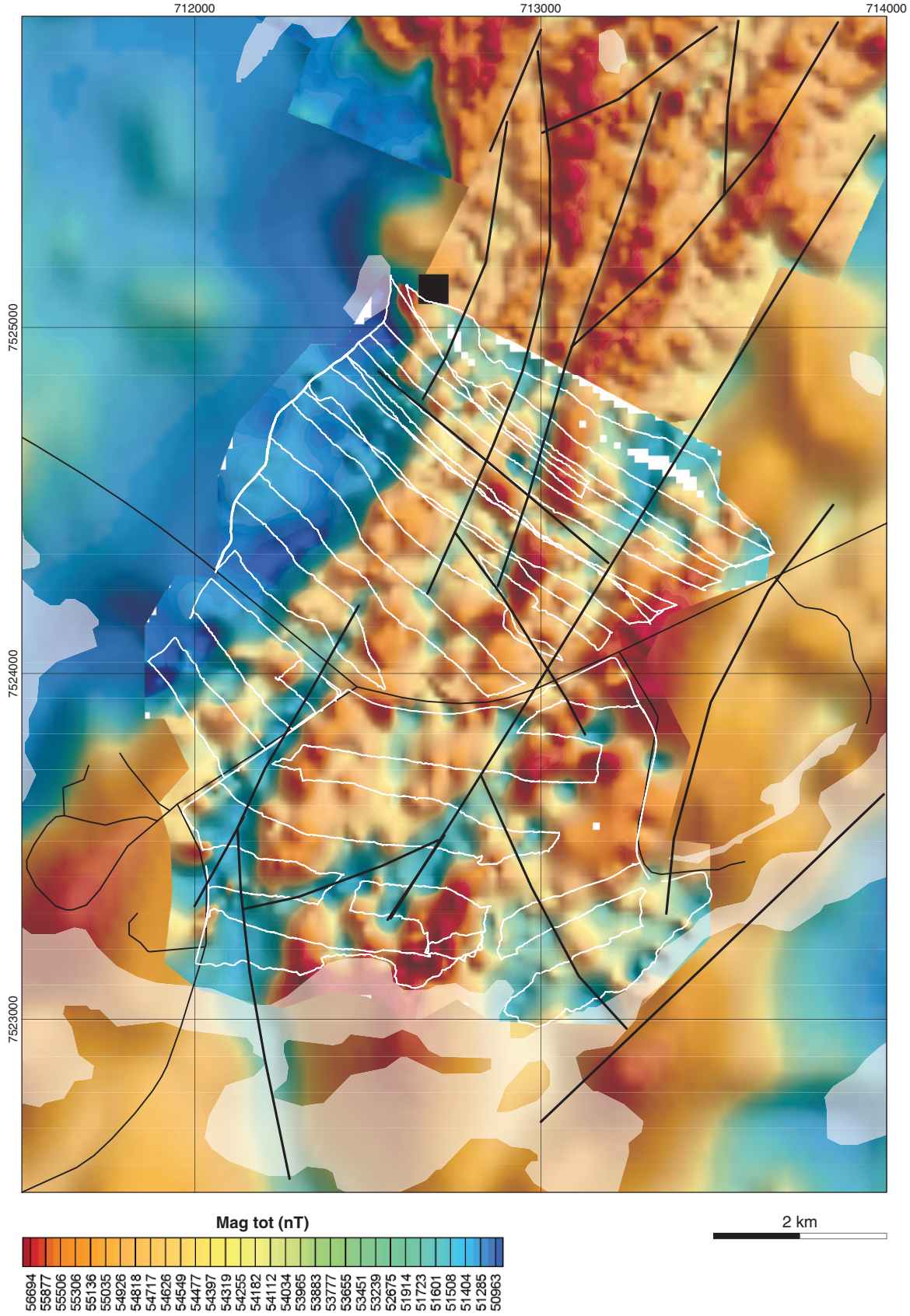

Figure 32. Magnetic map derived from 2013 ground measurements at Kaalasluspa area, southern Saarijärvi. White lines show ground measurement profiles. Thicker black lines are inferred deformation lineaments. Several black lines are roads.

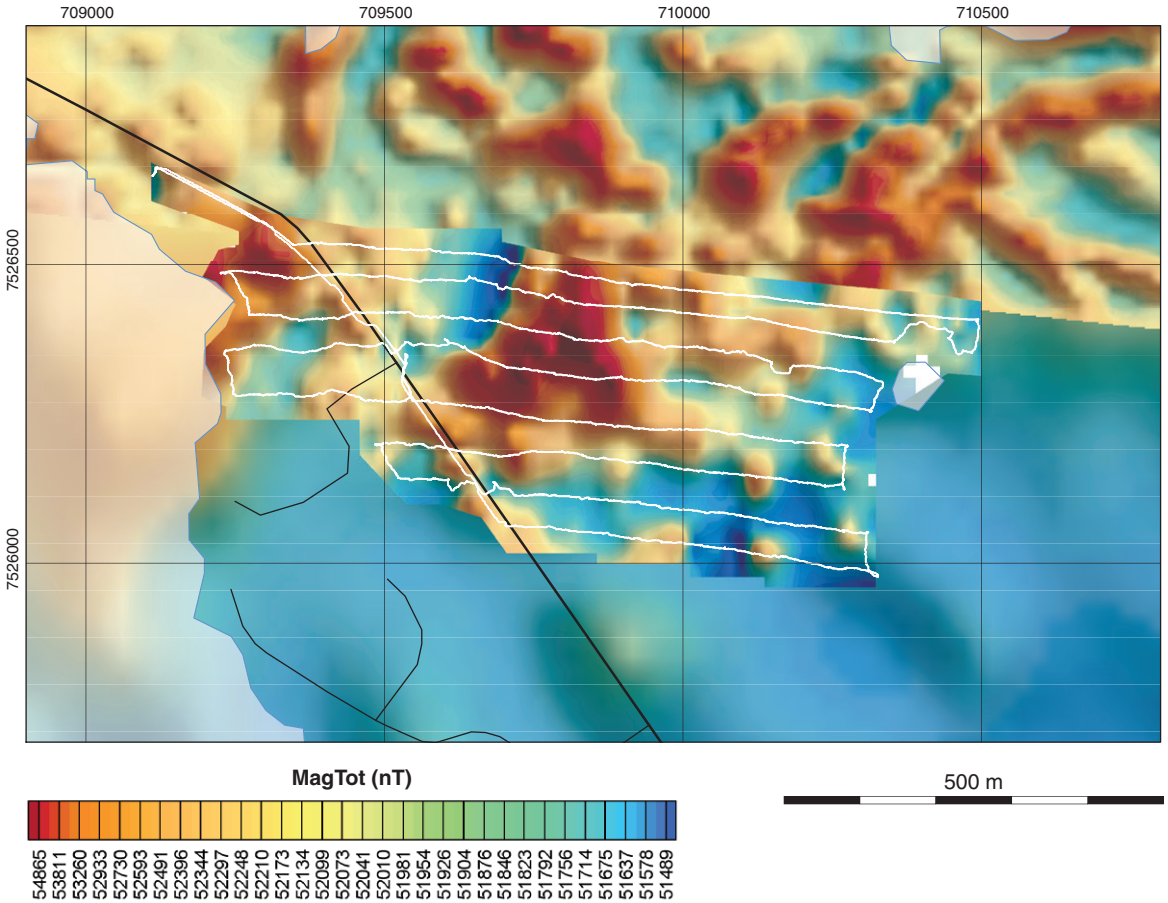

Figure 33. Ground magnetic anomaly map of the Archean stock located c. 1 km south-west of Lake Saarijärvi. White lines show ground magnetometer profiles. Roadways are also plotted.

Hand-held gamma spectrometer measurements and petrophysical sampling was conducted at two localities in Saarijärvi (Fig. 34). At a location underlain by the Archean syenitoid stock (7526447/709696, Fig. 25), spectrometer measurements showed potassium, uranium and thorium contents of 3.6%, 1.2 ppm and 18 ppm, respectively. At a location underlain by the larger Sevokarelian quartz alkali syenite (7524780/712020, Fig. 25), the spectrometer values were 5.3% potassium, 0.7 ppm uranium and 9 ppm thorium. The results are broadly similar for both intrusions and are within the same order of magnitude. This probably reflects the similar composition of these felsic intrusions and the variably developed potassic alteration.

FIELD ACTIVITIES IN THE TJÅRROJÅKKA AREA

The Tjårrojåkka key area is located approximately 50 km south-west of Kiruna (Figs. 1 and 21). The geology of the Tjårrojåkka key area is summarised in earlier SGU reports and maps by Geijer (1931), Ödman (1957), Offerberg (1967) and Witschard et al. (2004). The most detailed bedrock maps covering the area are two 1:50 000-scale sheets from SGUs Af and Ai map series. They are Af 3 (Offerberg 1967) in the west and Ai 198 (Witschard et al. 2004) in the east. A compilation of existing bedrock mapping, geochronology, geochemistry and geophysical data for the area is presented in Lynch & Berggren (2013).

The Tjårrojåkka key area is centered on a package of Svecokarelian (c. 2.0–1.84 Ga) metavolcanic rocks (basalt, andesite and rhyolite) assigned to the Porphyrite and Porphyry lithostrati-

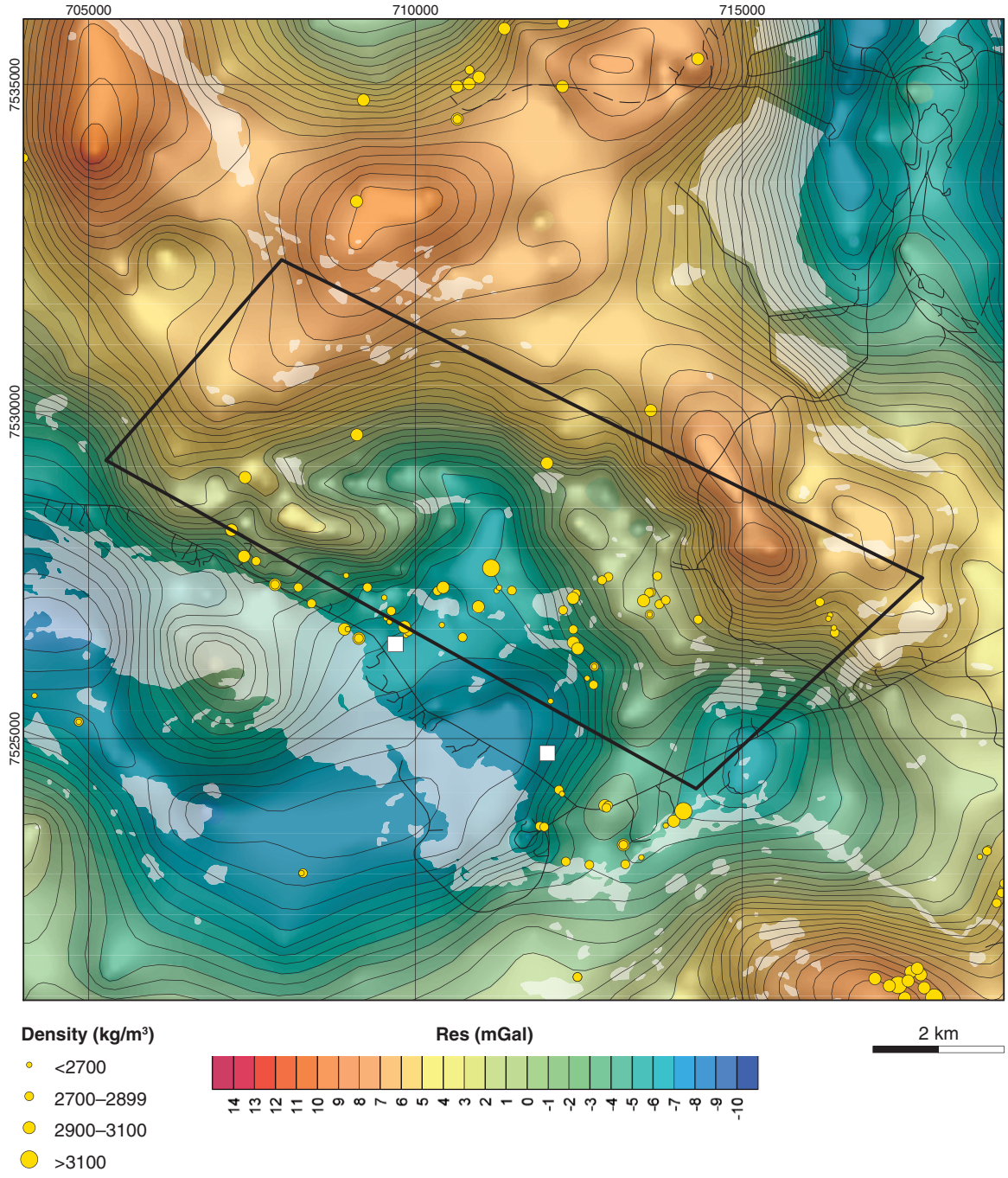

Figure 34. The gravity field of the Saarijärvi area. Yellow circles represent (by proportional size) densities of historical petrophysical samples. White squares are 2013 gamma spectrometry and petrophysical sampling locations. The isoline interval is 0.5 mGal.

graphic groups. The latter is also referred to as the Kiirunavaara group or Kiruna porphyries (see Table 2 in Bergman et al. 2001). The volcanic sequence is generally considered to both young and become more felsic from west to east, although local and regional deformation has complicated the stratigraphy (cf. Offerberg 1967, Bergman et al. 2001, Edfelt 2003). Svecokarelian intrusive rocks (c. 1.89–1.86 Ga) also occur in the area and primarily consist of quartz monzonitoids, syenitoids and granitoids of the Perthite-monzonite intrusive suite (e.g. Witschard 1984). Minor metagabbroid intrusives with an affinity to the Haparanda suite of plutons are also pre-

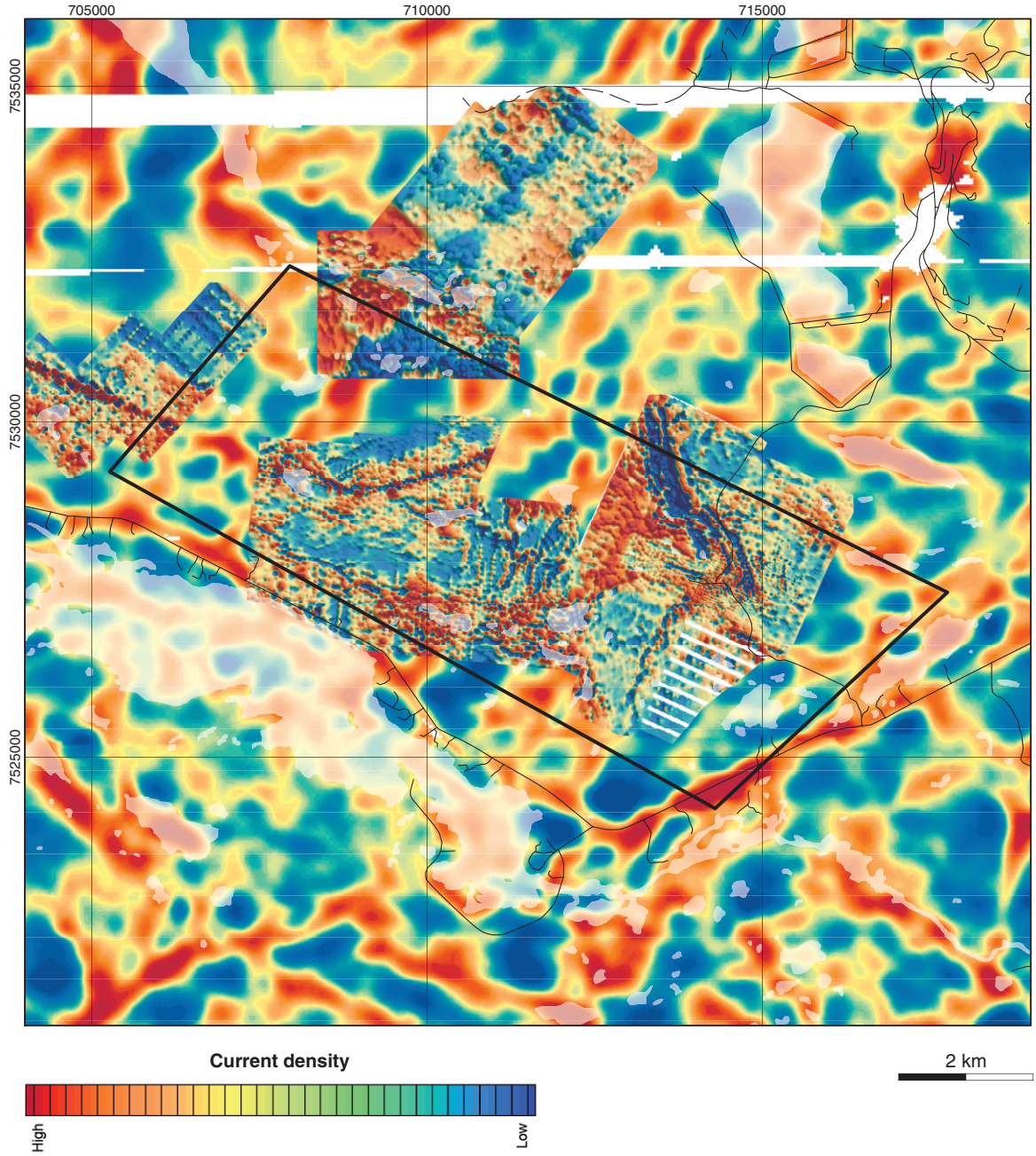

Figure 35. Combined airborne (current density) and ground (slingram) electromagnetic VLF map of the Saarijärvi area. For the airborne data, red indicates good conductivity. For the ground data, blue represents good conductivity.

sent. The area is best known for iron and copper-gold mineralization (IOCG-style) occurring at the Tjårrojåkka deposit (c. 56 million tonnes combined, e.g. Ros 1979, Frietsch 1997, Edfelt et al. 2005, Sandrin & Elming 2006).

During 2013, reconnaissance-level field sampling was conducted across the Tjårrojåkka key area with access provided by helicopter. While observation and sampling time was somewhat restricted for logistical reasons, several key locations were visited, providing an opportunity to sample some key stratigraphic horizons. Ongoing geochronology, petrography and geochemical studies will be conducted on the sampled material. Ground magnetic surveying was performed

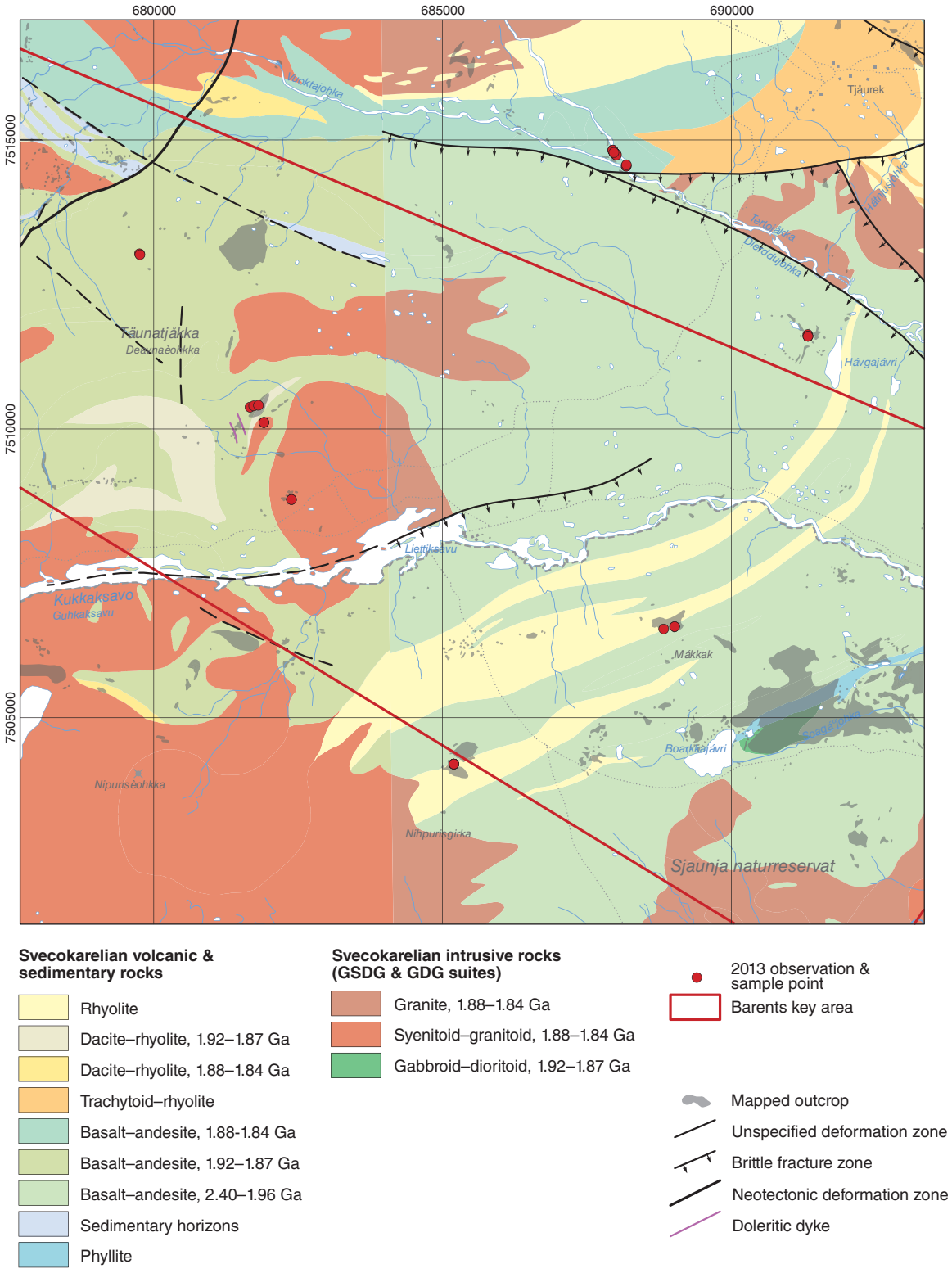

Figure 36. Bedrock geology of the Tjårrojåkka area showing the location of field observation and sample locations in 2013. Based on SGU's local bedrock database (1:50 000).

at one location to measure the magnetic signature of a system of magnetite-bearing veins hosted within an altered intermediate intrusive rock (discussed below).

Reconnaissance sampling of Svecokarelian volcanic and intrusive rocks

In total, eight localities within the Tjårrojåkka area were visited (Fig. 36). Two areas represented horizons of porphyritic rhyolite assigned to the Porphyry group (Bergman et al. 2001). Here, the rock is pinkish grey to reddish pink (altered?), massive, with a porphyritic texture consisting of medium to coarse-grained (c. 2–12 mm) plagioclase phenocrysts in a fine-grained (c. 0.1–0.5 mm) quartz- and feldspar-rich matrix (Fig. 37a–b). It occurs within planar, laterally continuous and parallel beds varying between 0.1 and 2.5 m in thickness. Measured magnetic susceptibility values ranged from 1390 to 2 230 × 10^{-5} SI, with an average value of 1 626 × 10^{-5} SI (n=8).

Basaltic rocks (basaltic andesite tuff?) assigned to the Porphyry group were also sampled (Fig. 36). At one location (7506572/689014), the rock is a relatively fresh, dark grey, massive, intercrystalline, fine-grained (c. 0.1–0.5 mm) basalt containing essential plagioclase and pyroxene (Fig. 37c–d). It occurs within c. 0.2–2 m thick flow beds that strike generally east–west. Quartz veining and fracture planes containing sulphide are locally present. In contrast, at another location closer to a regional deformation zone (7511603/691324), the basalt displays relatively intense scapolite-actinolite-magnetite alteration along with localised zones of reddish-pink potassic (K-feldspar) staining and disrupted volcanic clasts associated with magnetite. Measured magnetic susceptibility values of basalt outcrops ranged from 39 to 12 200 × 10^{-5} SI, with an average value of 4 463 × 10^{-5} SI (n=16).

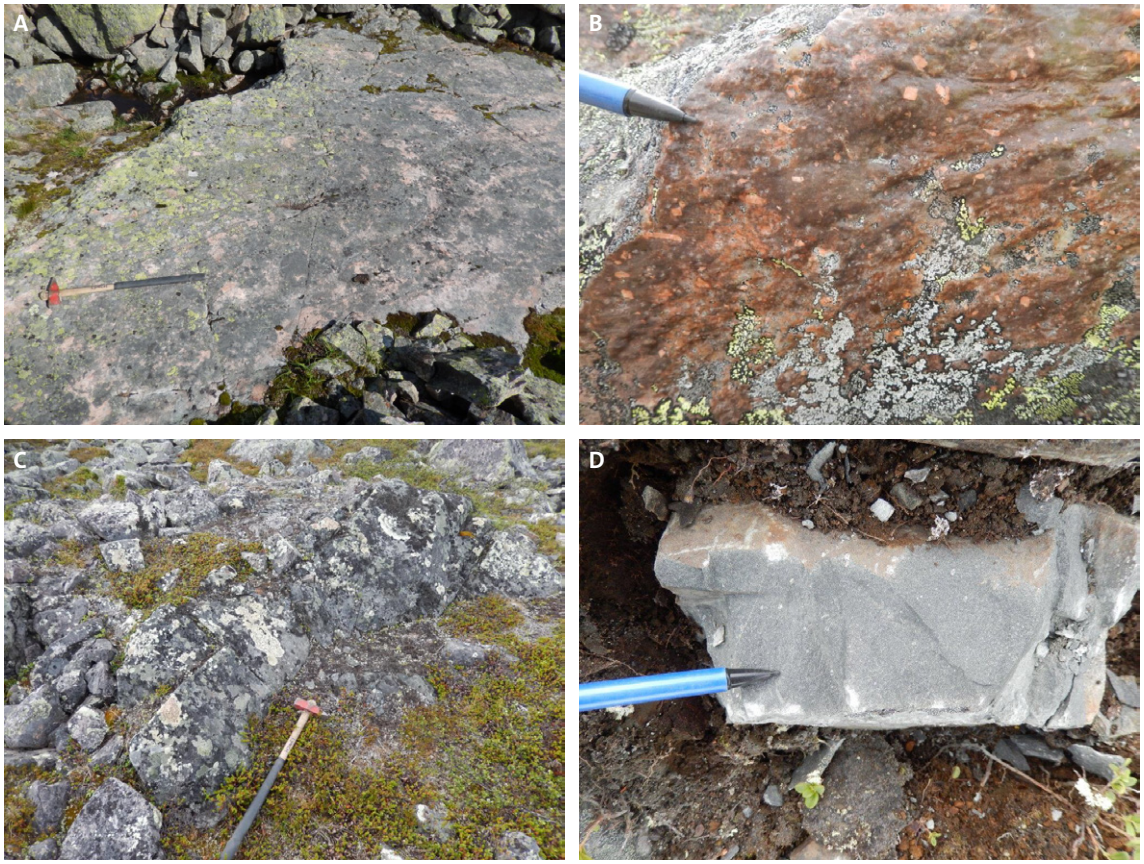

Figure 37. Volcanic rocks at Tjårrojåkka. **A–B.** Rhyolitic volcanic rocks containing plagioclase feldspar phenocrysts (7504203/685197). **C–D.** Thickly bedded, crystalline, basaltic tuff (7506578/689014).

Additional observations and sampling of granitoid rocks within the central part of the Tjårrojåkka key area were also undertaken (Fig. 36). Here, several felsic intrusions occur that have compositions ranging from granodiorite to alkali feldspar granite. The visited intrusions are also spatially associated with regional-scale magnetic anomalies (Fig. 39). The aim of this sampling was to provide material for geochronology work and to complement the investigation of intrusive rocks in the Saarijärvi area.

Geological and geophysical characteristics of a magnetite-bearing vein system

Approximately 2 km to the north of the Tjårrojåkka key area, where the Kirjasjåkka and Vuoktajohka rivers join, a newly discovered zone of altered rock containing an amphibole-magnetite vein system was investigated (Fig. 38). The area occurs within a regional, ductile deformation zone that has a predominant north-west orientation (Fig. 39). A preliminary lineament interpretation of the area's regional magnetic signature indicates additional east-north-east orientated zones of deformation.

The host rock in the area is a dioritoid body displaying intense, pervasive, scapolite-albite alteration. It is cross-cut by several dark grey to greenish grey, planar to wavy, sub-parallel amphibole (actinolite?) veins containing variable amounts of disseminated and patchy magnetite. The veins vary from c. 1 cm to 1 m in thickness (Fig. 38a–b). Albite±scapolite veinlets also occur in the area and they appear to both cross-cut and be cut by the actinolite-magnetite veins

Figure 38. Amphibole-magnetite veining in the Tjårrojåkka area (7514809/687956). **A–B.** Amphibole-magnetite-albite veins cross-cutting a scapolite-albite altered intermediate (dioritic?) rock. **C–D.** Albite veining associated with amphibole-magnetite veins. Late-stage epidote±carbonate(?) veining overprinting in D.

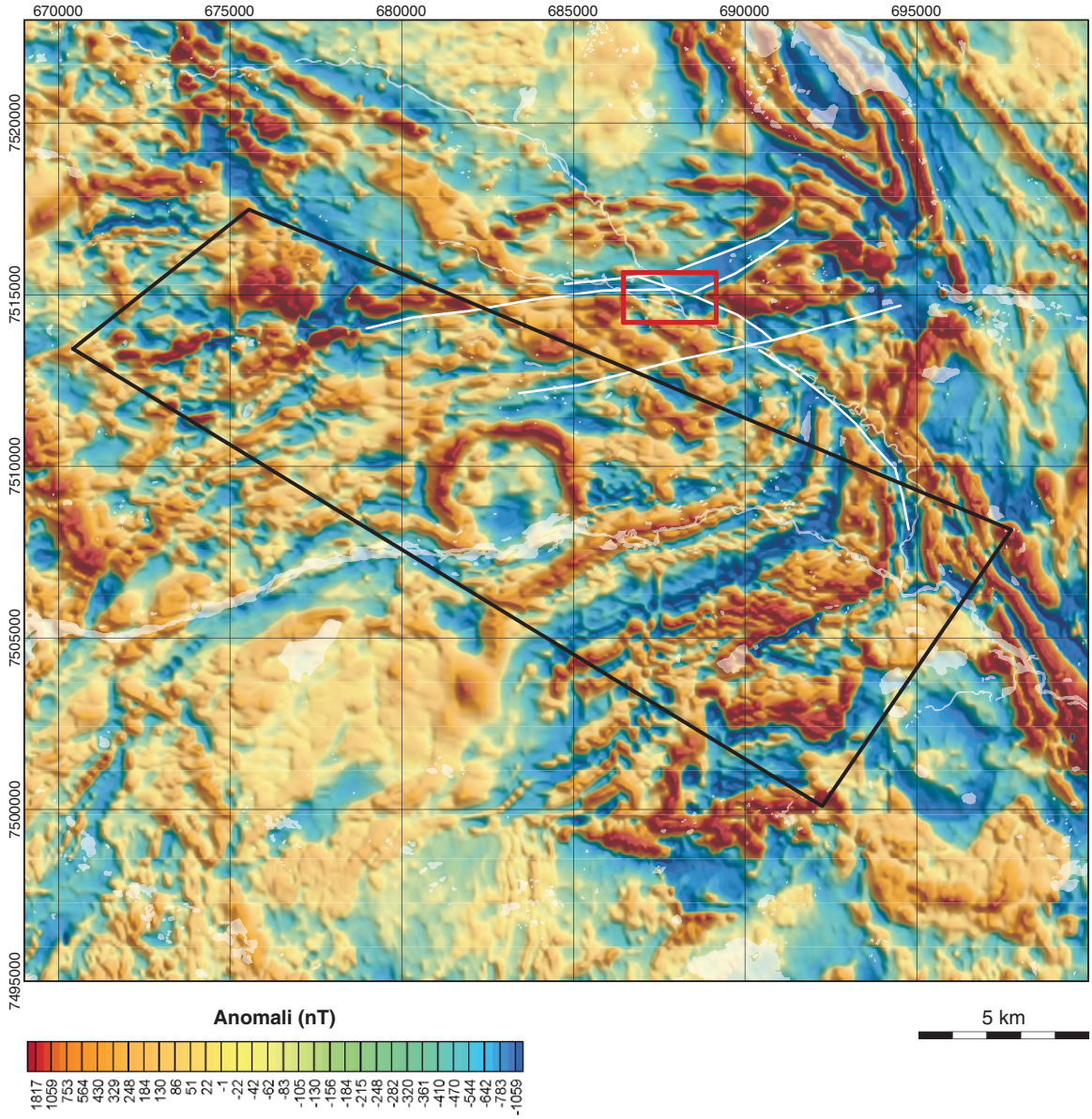

Figure 39. Magnetic anomaly map of the Tjårrojåkka area. Geophysical fieldwork during 2013 was carried out within the highlighted rectangular area. Plotted lineaments represent inferred deformation zones in the vicinity.

(Fig. 38c). Late-stage epidote-carbonate patches and veining associated with orange pink K-feldspar staining also occur in the area (Fig. 38d).

The result of a ground magnetometer survey of the area that hosts the magnetite-bearing veins is shown in Figure 40. The purpose of the survey was to map the spatial extent of the vein system and delineate the magnetically anomalous zone. During this survey, the largest field strength recorded by the magnetometer was 88000 nT from an area close to the bank of the eastern river (7514750/687970). The mapped magnetic field shows a linear, positive magnetic anomaly zone with an east to east-norh-east orientation. This zone coincides with the location of the magnetite-bearing veins and also corresponds to the general orientation of the regional-scale deformation zone that transects the area (see Fig. 39).

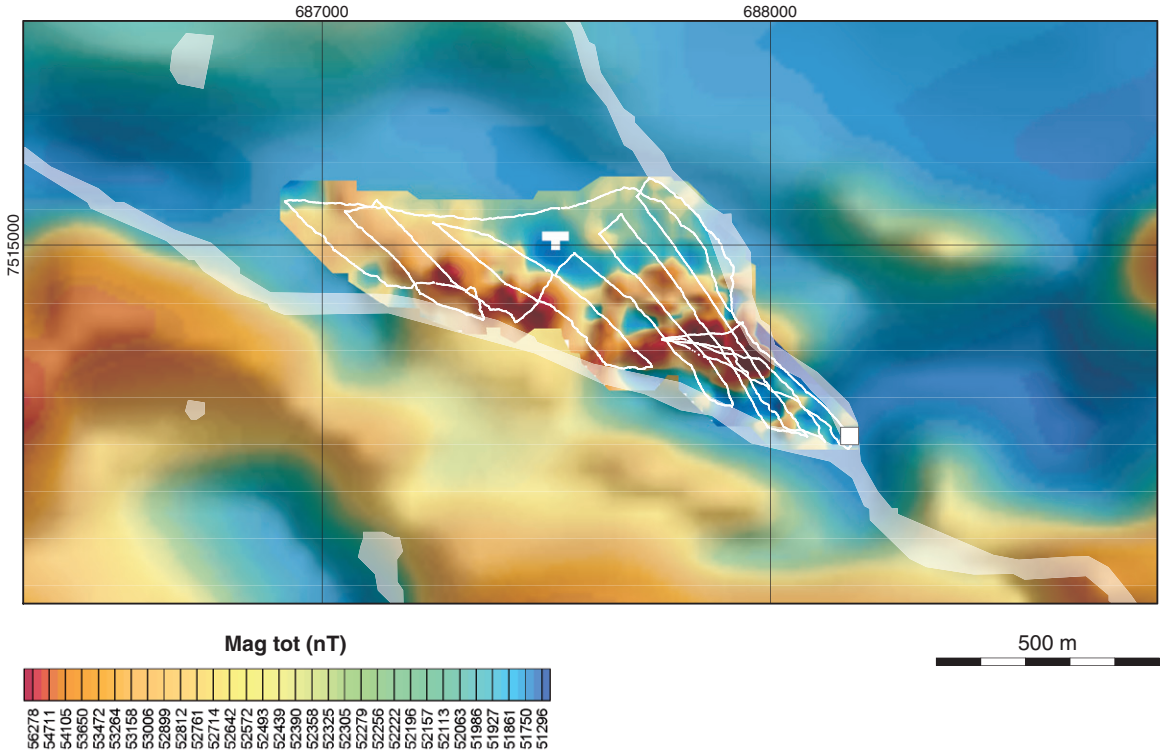

Figure 40. Ground magnetic map of the study area. The background anomalies represent airborne measurements. White squares represent gamma spectrometery and petrophysical sampling locations.

Several gamma spectrometer measurements were also carried out in the area, along with the acquisition of a petrophysical sample (Fig. 40). Hand-held spectrometer measurements were 1.5% potassium, 1.5 ppm uranium and 1.8 ppm thorium for the altered dioritoid rock that hosts the magnetite-bearing veins. Magnetic ssusceptibility values up to $7\,700 \times 10^{-5}$ SI were also measured in this area.

REFERENCES

Bergman, J., 1993: Tectonic studies in the Saarijärvi–Pahtohavare area. *In* O. Martinsson, J.A. Perdahl & J. Bergman: Greenstone and porphyry hosted ore deposits in northern Norrbotten. *PIM/NUTEK report #1, Luleå, MINK 95117*, 77 p.

Bergman, S., Kubler, L. & Martinsson, O., 2000: Regional geological and geophysical maps over northern Norrbotten County: Bedrock map. *Sveriges geologiska undersökning Ba 56:1.*

Bergman, S., Kubler, L. & Martinsson, O., 2001: Description of regional geological and geophysical maps of northern Norbotten County. *Sveriges geologiska undersökning Ba 56*, 110 pp.

Billström, K., Eilu, P., Martinsson, O., Niiranen, T., Broman, C., Weihed, P., Wanhainen, C. & Ojala, J., 2010: IOCG and related mineral deposits of the northern Fennoscandian Shield. *In* T.M. Porter (ed.): *Hydrothermal iron oxide-copper-gold & related deposits: a global perspective, vol. 3. Advances in the understanding of IOCG deposits*. PGC Publishing, Adelaide. 381–414.

Carlon, C.J., 2000: Iron oxide systems and base metal mineralisation in northern Sweden. *In* T.M.Porter (ed.): *Hydrothermal iron oxide copper gold and related deposits: A global perspective*. Australian Mineral Foundation, 283–296.

Edfelt, Å., 2003: *Geology, alterations, and mineral chemistry of the Tjårrojåkka Fe-oxide Cu–Au occurrences, N Sweden*. Unpublished MSc thesis, Luleå University.

Edfelt, Å., Armstrong, R.N., Smith, M. & Martinsson, O., 2005: Alteration paragenesis and mineral chemistry of the Tjårrojåkka apatite–iron and Cu (-Au) occurrences, Kiruna area, northern Sweden. *Mineralium Deposita 40*, 409–434.

Eriksson, B. & Hallgren, U., 1975: Beskrivning till berggrundskartbladen Vittangi NV, NO, SV, SO. *Sveriges geologiska undersökning Af 13–16*, 203 pp.

Frietsch, R., 1997: The iron ore inventory programme 1963–1972 in Norrbotten County. *Sveriges geologiska undersökning Rapporter och meddelanden 92*, 77 pp.

Geijer, P., 1918: Det grafit- och järnmalmsförande området vid Vittangi. *Sveriges geologiska undersökning C 284,* 104 pp.

Geijer, P., 1931: The iron ores of the Kiruna type. Geographical distribution, geological characters and origin. *Sveriges geologiska undersökning C 367*, 39 pp.

Gerdin, P., Johansson, L., Hansson, K.-E., Holmqvist, A. & Ottosson, D., 1990: Grafit – uppslagsgenerering i Norrbotten 1990. *Sveriges geologiska undersökning Prap 90068*, 100 pp.

Gustafsson, B., 1993: The Swedish Norrbotten greenstone belt: a compilation of available information concerning exploration. *NSG report no. 93003*, 52 pp.

Jensen, L.S., 1976: A new cation plot for classifying subalkalic volcanic rocks. *Ontario Division of Mines, Miscellaneous Paper 66*, 1–21.

Kumpulainen, R.A., 2000: *The Paleoproterozoic sedimentary record of northernmost Norrbotten, Sweden*. Unpublished report for Sveriges geologiska undersökning, Stockholm University.

Lager, I. & Loberg, B., 1990: *Sedimentologisk bassänganalytisk malmprospekteringsmetodik inom norrbottniska grönstensbälten*. STU-projekt 86-03967P, Luleå, 131 pp.

Lundqvist, T., 1979: The Precambrian of Sweden. *Sveriges geologiska undersökning C 366*, 87 pp.

Lynch, E.P. & Berggren, R., 2013: Background information Tjårrojåkka key area (29I Kebnekaise SO & 29J Kiruna SV). *Sveriges geologiska undersökning SGU-rapport 2013:14*, 43 pp.

Lynch, E.P. & Jönberger, J., 2013a: Summary report on the geological and geophysical characteristics of the Nunasvaara key area (29K Vittangi NO & SO). *Sveriges geologiska undersökning SGU-rapport 2013:11*, 35 pp.

Lynch, E.P. & Jönberger, J., 2013b: Summary report on the geological and geophysical characteristics of the Saarijärvi key area (29J Kiruna NO, NV, SO). *Sveriges geologiska undersökning SGU-rapport 2013:10*, 48 pp.

Martinsson, O., 1993: Greenstone and porphyry hosted ore deposits in northern Norrbotten. *PIM/NUTEK report #1, Luleå, MINK 95117*, 77 pp.

Martinsson, O., 1995: Greenstone and porphyry hosted ore deposits in northern Norrbotten. *PIM/NUTEK report #3*, 58 p.

Martinsson, O., 1997: *Tectonic setting and metallogeny of the Kiruna greenstones*. PhD thesis, Luleå University.

Martinsson, O. & Wanhainen, C., 2000: *2nd annual GEODE-Fennoscandian shield field workshop on Palaeoproterozoic and Archaean greenstone belts and VMS districts in the Fennoscandian Shield*. Workshop excursion guide.

Martinsson, O. & Wanhainen, C., 2013: Fe oxide and Cu-Au deposits in the northern Norrbotten ore district. *SGA excursion guidebook SWE5*, 74 pp.

Offerberg, J., 1967: Beskrivning till berggrundskartbladen Kiruna NV, NO, SV, SO. *Sveriges geologiska undersökning Af 1–4*, 146 pp.

Offerberg, J. & Nilsson, G., 1967: Bergrundskartan 29J Kiruna NV, NO, SV, SO. *Sveriges geologiska undersökning Af 1–4.*

Ödman, O.H., 1957: Beskrivning till berggrundskartbladen över urberget i Norrbottens län. *Sveriges geologiska undersökning Ca 41*, 151 pp.

Pearce, J.A., 1996: A user's guide to basalt discrimination diagrams. *In* D.A. Wyman (ed.): Trace element geochemistry of volcanic rocks: applications for massive sulphide exploration. *Geological Association of Canada, Short Course Notes 12*, 79–113.
Ros, F., 1979: Tjårrojåkka kopparmalmsfyndighet. *Sveriges geologiska undersökning BRAP 82567*, 13 pp.
Sandrin, A. & Elming, S.Å., 2006: Geophysical and petrophysical study of an iron oxide copper gold deposit in northern Sweden. *Ore Geology Review 29*, 1–18.
Shaikh, N.A., 1972: Sammanställning över grafitförekomsterna i det centrala Vittangifältet, Norrbotten län. *Sveriges geologiska undersökning Brap 00876*, 20 pp.
Skiöld, T. & Page, R.W., 1998: SHRIMP and isotope dilution zircon ages on Archean basement-cover rocks in north Sweden. *Nordiske Geologiske Vintermöte abstract volume, Århus*, 273.
Smith, M., Coppard, J., Herrington, R. & Stein, H., 2007: The geology of the Rakkurijärvi Cu–(Au) prospect, Norrbotten: a new iron-oxide–copper–gold deposit in northern Sweden. *Economic Geology 102*, 393.
Smith, M.P., Storey, C.D., Jefferies, T.E. & Ryan, C., 2009: In situ U–Pb and trace element analysis of accessory minerals in the Kiruna district, Norrbotten, Sweden: New constraints on the timing and origin of mineralization. *Journal of Petrology 50*, 2063.
Smith, M., Coppard, J. & Herrington, R., 2010: The geology of the Rakkurijärvi copper-prospect, Norrbotten county, Sweden. *In* T.M. Porter (ed.): *Hydrothermal iron oxide copper–gold and related deposits: a global perspective 4*. PGC Publishing, Adelaide. 427–440.
Stephens, M.B. & Weihed, P., 2013: Tectonic evolution and mineral resources in the Fennoscandian Shield, Sweden. *In* O. Martinsson & C. Wanhainen (eds.): Fe oxide and Cu-Au deposits in the northern Norrbotten ore district. *SGA excursion guidebook SWE5*, 8–18.
Storey, C.D., Smith, M.P. & Jefferies, T.E., 2007: In situ LA-ICP-MS U–Pb dating of metavolcanics of Norrbotten, Sweden: records of extended geological histories in complex titanite grains. *Chemical Geology 240*, 163.
Weihed, P., Arndt, N., Billström, K., Duchesne, J.-C., Eilu, P, Martinsson, O, Papunen, H & Lahtinen, R., 2005: Precambrian geodynamics and ore formation: The Fennoscandian Shield. *Ore Geology Reviews 27*, 273.
Witschard, F., 1984: The geological and tectonic evolution of the precambrian of Northern Sweden – a case for basement reactivation? *Precambrian Research 23*, 273.
Witschard, F., Thelander, T., Kübler, L., Stölen, L.K. & Perdahl, J.A., 2004: Berggrundskartan 29I Kebnekaise SO. *Sveriges geologiska undersökning Ai 198*.